Journal of Medicinal Chemistry

Article

pubs.acs.org/jmc

Discovery of Allosteric Modulators of Factor XIa by Targeting Hydrophobic Domains Adjacent to Its Heparin-Binding Site

Rajesh Karuturi,[†] Rami A. Al-Horani,[†] Shrenik C. Mehta,[†] David Gailani,[‡] and Umesh R. Desai*[,†]

[†]Department of Medicinal Chemistry and Institute for Structural Biology and Drug Discovery, Virginia Commonwealth University, Richmond, Virginia 23298, United States

[‡]Departments of Pathology, Immunology and Microbiology, Vanderbilt University Medical Center, Nashville, Tennessee 37203, United States

Supporting Information

ABSTRACT: To discover promising sulfated allosteric modulators (SAMs) of glycosaminoglycan-binding proteins (GBPs), such as human factor XIa (FXIa), we screened a library of 26 synthetic, sulfated quinazolin-4(3H)-ones (QAOs) resulting in the identification of six molecules that reduced the V_{max} of substrate hydrolysis without influencing the K_M. Mutagenesis of residues of the heparin-binding site (HBS) of FXIa introduced a nearly 5-fold loss in inhibition potency supporting recognition of an allosteric site. Fluorescence studies showed a sigmoidal binding profile indicating highly cooperative binding. Competition with a positively charged, heparin-binding polymer did not fully nullify inhibition suggesting importance of hydrophobic forces to binding. This discovery suggests the operation of a dual-element recognition process, which relies on an initial Coulombic attraction of anionic SAMs to the cationic HBS of FXIa that forms a locked complex through tight interaction with an adjacent hydrophobic patch. The dual-element strategy may be widely applicable for discovering SAMs of other GBPs.

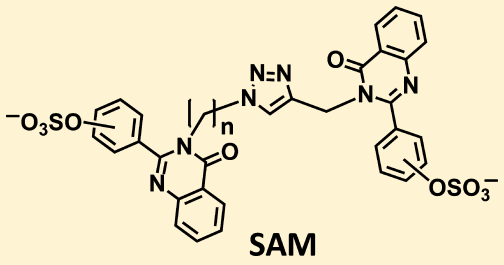

INTRODUCTION

Glycosaminoglycan (GAG)-binding proteins (GBPs) play critical roles in a number of physiological and pathological responses such as coagulation, immune regulation, angiogenesis, morphogenesis, viral infection, and cancer.[1−4] The modulation of these responses by GAGs such as heparin, heparan sulfate (HS), and chondroitin sulfate offers major opportunities for discovering a large number of therapeutic agents considering that GAGs present a wide range of structures for protein recognition. Yet, only one interaction, the heparin−antithrombin interaction,[5] has yielded a clinically useful agent.

A major problem in discovering GAG-based molecules, for example, heparin oligomers, as drugs is the rather poor specificity of their interaction with proteins.[6−8] Although the presence of certain rare residues in heparin/heparan sulfate (H/HS) chains, such as 3-*O*-sulfated glucosamine or 2-*O*-sulfated glucuronic acid, is believed to indicate specificity, the majority of HS−protein interactions are likely to be nonselective because the nature of forces that govern these interactions is primarily electrostatic, which is nondirectional and operational over long distances.[8,9] This implies that H/HS recognize practically any collection of electropositive residues, that is, a group of arginines and lysines, which severely limits the discovery of highly selective modulators.

A number of researchers have attempted the design of H/HS mimetics that rely on a limited number of anionic groups (e.g., sulfate, carboxylate, phosphate) on a smaller saccharide scaffold to alleviate the difficulties of nonspecificity of H/HS polymers. Examples of these include oligosaccharides containing sulfate[10−13] and phosphate[14] groups, aptamers,[15] sulfated-linked cyclitols,[16] and dendritic polyglycerol sulfates.[17] Although none has reached the clinic as yet, a pentaphosphate oligosaccharide called PI-88 is being evaluated in several clinical trials.

Another concept being advanced to capitalize on the possibility of numerous druggable GAG−protein interactions is sulfate-decorated nonsaccharide small molecules. These include sulfated flavans[18,19] and flavones,[20−22] sulfated xanthones,[23] and sulfated tetrahydroisoquinolines.[24,25] Sulfated flavans were the first small, nonsugar molecules designed utilizing a de novo structure-based approach to modulate antithrombin function.[18,19] In contrast, a pharmacophore-based approach was used to design sulfated isoquinolines,[24,25] while the rest were investigated as analogues of the parent sulfated flavans. Although promising, the affinity of most of the designed, sulfated, nonsaccharide, small molecules was found to be high (>250 μM).[18−25]

Despite these advances, the field suffers severely from the lack of a generalizable strategy for the rational design of modulators of GAG−protein interactions. In fact, no real "design" has been utilized in developing the polymeric polyanions,[9−16] while the computational design of sulfated, small molecule antithrombin activators[18,24] is highly case-specific. A rational, more broadly applicable strategy would

Received: November 28, 2012

   dx.doi.org/10.1021/jm301757v | *J. Med. Chem.* XXXX, XXX, XXX−XXX

greatly help in developing selective sulfated modulators of GBPs.

We recently studied the mechanism of inhibition of human α-thrombin by sulfated benzofurans,[26] small functional mimetics of GAGs, and found that these molecules recognize a single arginine residue that is located adjacent to a hydrophobic domain.[27] This gave rise to the possibility of designing molecules that specifically target the hydrophobic (hP) domain surrounding the heparin-binding site (HBS) of proteins. In fact, coagulation enzymes possess hP domains of varying sizes around their strongly electropositive HBSs. For example, thrombin contains two clusters of hP residues near its HBS,[27,28] while the corresponding site in factor XIa is significantly different. Thus, we reasoned that it should be possible to discover molecules, herein called as sulfated allosteric modulators (SAMs), by exploiting differential recognition of hP patches around the HBS. We reasoned that the strategy would involve (1) initial attraction of an anionic sulfate group present on a SAM to one or more arginines/lysines present in the HBS of a heparin-binding protein (HBP) followed by (2) recognition of an adjacent hP patch on the HBP to form a complex (Figure 1). Enzymes devoid of either

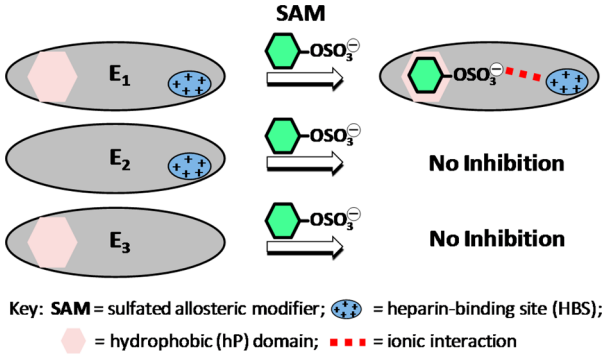

Figure 1. Strategy for the design of a SAM of a GBP exploiting the difference in hydrophobicity (hP, shown as light colored patch) on the periphery of a HBS (shown as blue ellipse with positive charges). A SAM binds an enzyme (shown by red dashed line), e.g., E1, only if it contains both hP and HBS. E2 and E3 do not recognize the SAM because of an absence of either hP or HBS. This generates selectivity of recognition.

the HBS or the hP domain would not bind the SAM and hence escape inhibition. Only enzymes possessing the HBS and an appropriate hP domain will be targeted by SAMs. The potency of inhibition will be dependent on the complementarity of SAM's hydrophobic scaffold with the hP domain on the enzyme. In essence, this strategy revolves around electronic steering of a small molecule to the HBS of the protein due to nondirectionality of an initial, weak ionic bond followed by filtering and tight locking of an optimal hydrophobic SAM scaffold. This work describes that success of this strategy in the discovery of SAMs of human factor XIa.

EXPERIMENTAL PROCEDURES

Chemicals, Reagents, and Analytical Chemistry. Anhydrous CH_2Cl_2, THF, CH_3CN, DMF, DMA, and acetone were purchased from Sigma–Aldrich (Milwaukee, WI) or Fisher (Pittsburgh, PA) and used as such. Other solvents used were of reagent gradient and used as purchased. Analytical thin layer chromatography (TLC) was performed using UNIPLATE silica gel GHLF 250 μm precoated plates (ANALTECH, Newark, DE). Column chromatography was performed using silica gel (200–400 mesh, 60 Å) from Sigma–Aldrich. Chemical reactions sensitive to air or moisture were carried out under nitrogen atmosphere in oven-dried glassware. Reagent solutions, unless otherwise noted, were handled under a nitrogen atmosphere using syringe techniques. Flash chromatography was performed using the Teledyne ISCO (Lincoln, NE) Combiflash RF system and disposable normal silica cartridges of 30–50 μm particle size, 230–400 mesh size, and 60 Å pore size. The flow rate of the mobile phase was in the range 18–35 mL/min, and mobile phase gradients of ethyl acetate/hexanes and CH_2Cl_2/CH_3OH were used to elute compounds.

Proteins and Chromogenic Substrates. Human plasma proteases including thrombin, factor Xa, factor IXa, factor XIa, and active-site labeled FXIa, that is, FXIa-DEGR, were obtained from Haematologic Technologies (Essex Junction, VT). Bovine α-chymotrypsin and bovine trypsin were obtained from Sigma–Aldrich (St. Louis, MO). Stock solutions of factor XIa, thrombin, trypsin, and chymotrypsin were prepared in 50 mM Tris–HCl buffer, pH 7.4, containing 150 mM NaCl, 0.1% PEG8000, and 0.02% Tween80. Stock solutions of factor Xa were prepared in 20 mM Tris–HCl buffer, pH 7.4, containing 100 mM NaCl, 2.5 mM $CaCl_2$, 0.1% PEG8000, and 0.02% Tween80. Chromogenic substrates, Spectrozyme TH (H-*D*-cyclohexylalanyl-Ala-Arg-*p*-nitroanilide), Spectrozyme factor Xa (Methoxycarbonyl-*D*-cyclohexylglycyl-Gly-Arg-*p*-nitroanilide), and Spectrozyme CTY were obtained from American Diagnostica (Greenwich, CT). Factor XIa chromogenic substrate (S-2366, L-PyroGlu-Pro-Arg-*p*-nitroanilide·HCl) and trypsin substrate (S-2222, Benzoyl-Ile-Glu(γ-OH and -OCH_3)-Gly-Arg-*p*-nitroanilide·HCl) were obtained from Diapharma (West Chester, OH). Bovine unfractionated heparin (UFH) was purchased from Sigma–Aldrich (St. Louis, MO). Pooled normal human plasma for coagulation assays was purchased from Valley Biomedical (Winchester, VA). Activated partial thromboplastin time reagent containing ellagic acid, thromboplastin-D, and 25 mM $CaCl_2$ was obtained from Fisher Diagnostics (Middletown, VA).

Chemical Characterization of Compounds. ^1H and ^{13}C NMR were recorded on a Bruker-400 MHz spectrometer in either $CDCl_3$, CD_3OD, acetone-d_6, DMSO-d_6, or D_2O. Signals, in parts per million (ppm), are either relative to the internal standard or to the residual peak of the solvent. The NMR data are reported as chemical shift (ppm), multiplicity of signal (s = singlet, d = doublet, t = triplet, q = quartet, dd = doublet of doublet, m = multiplet), coupling constants (Hz), and integration. Electrospray ionization mass spectrometry (ESI-MS) of compounds were recorded using a Waters Acquity TQD MS spectrometer in positive or negative ion modes. Samples were dissolved in methanol and infused at a rate of 20 μL/min. For high-resolution MS (HRMS) measurements, a Perkin–Elmer AxION 2 TOF MS was used in negative ion mode. Ionization conditions on both instruments were optimized for each compound to maximize the ionization of the parent ion. Generally, the extractor voltage was set to 3 V, the Rf lens voltage was 0.1 V, the source block temperature was set to 150 °C, and the desolvation temperature was about 250 °C. The purity of each final compound was greater than 95% as determined by ultraperformance liquid chromatography–mass spectrometry (UPLC-MS).

General Procedure for Synthesis of Sulfated Quinazolin-4(3H)-ones. Sulfation of phenolic precursors was achieved using microwave-assisted chemical sulfation as described earlier.[29,30] Briefly, to a stirred solution of polyphenol in anhydrous CH_3CN (1–5 mL) at room temperature, Et_3N (10 equiv per –OH group) and Me_3N/SO_3 complex (6 equiv per –OH) were added. The reaction vessel was sealed and microwaved (CEM Discover, Cary, NC) for 30 min at 90 °C. The reaction mixture was cooled and transferred to a round-bottom flask, and the volume was reduced as much as possible under low pressure conditions at 25 °C. The reaction mixture was then directly loaded on to a flash chromatography column and purified using a dichloromethane and methanol solvent system (5–20%) to obtain the sulfated quinazolin-4(3H)-ones (QAOs). The samples were concentrated and reloaded onto a SP Sephadex C-25 column for sodium exchange. Appropriate fractions were pooled, concentrated in vacuo, and lyophilized to obtain a white powder. Spectral character-

dx.doi.org/10.1021/jm301757v | J. Med. Chem. XXXX, XXX, XXX–XXX

istics of all the sulfated compounds **3aS**−**3gS**, **7S**−**20S**, and **25S**−**29S** are listed below. See the Supporting Information for details.

(3aS). ^{1}H NMR (D_2O, 400 MHz): 7.89−7.87 (m, 1H), 7.69−7.63 (m, 3H), 7.56−7.52 (m, 1H), 7.48−7.45 (m, 2H), 7.36 (t, J = 7.8 Hz, 1H). ^{13}C NMR (D_2O, 100 MHz): 151.41, 135.56, 133.50, 130.56, 127.52, 125.74, 125.40, 124.97, 120.78, 119.42. MS (ESI) calculated for $C_{14}H_9N_2NaO_5S$, $[(M - H)]^-$, m/z 339.01, found $[(M - Na)]^-$, m/z 317.17.

(3bS). ^{1}H NMR (DMSO-d_6, 400 MHz): 8.23 (d, J = 8.7 Hz, 1 H), 8.11 (m, 2 H), 7.66 (m, 2 H), 7.35 (m, 1 H), 7.26 (d, J = 8.8 Hz, 1 H), 6.87 (d, J = 8.7 Hz, 1 H). ^{13}C NMR (DMSO-d_6, 100 MHz): 170.5, 158.15, 139.1, 129.49, 128.64, 126.66, 125.73, 119.38, 115.09. MS (ESI) calculated for $C_{14}H_9N_2NaO_5S$, $[(M - H)]^-$, m/z 339.01, found $[(M - Na)]^-$, m/z 317.17.

(3cS). ^{1}H NMR (D_2O, 400 MHz): 8.13−8.11 (m, 1 H), 7.86−7.82 (m, 1 H), 7.72−7.68 (m, 3 H), 7.54 (t, J = 8.0 Hz, 1 H), 7.48 (t, J = 2.1 Hz, 1 H). ^{13}C NMR (D_2O, 100 MHz): 152.17, 135.76, 134.72, 127.81, 125.96, 118.56, 118.31. MS (ESI) calculated for $C_{14}H_8N_2Na_2O_9S_2$ $[(M - Na)]^-$, m/z 435.33, found $[(M - Na)]^-$, m/z 435.10.

(3dS). ^{1}H NMR (D_2O, 400 MHz): 7.96 (d, J = 8.0 Hz, 1H), 7.71 (t, J = 7.7 Hz, 1 H), 7.53 (d, J = 8.2 Hz, 1 H), 7.47−7.35 (m, 4 H), 3.90 (s, 3 H). ^{13}C NMR (100 MHz, D_2O): 151.45, 142.88, 135.63, 130.40, 127.48, 125.86, 122.82, 120.64, 119.49, 112.57, 56.27. MS (ESI) calculated for $C_{15}H_{11}N_2NaO_6S$ $[(M - Na)]^-$, m/z 347.31, found $[(M - Na)]^-$, m/z 347.16.

(3eS). ^{1}H NMR (D_2O, 400 MHz): 7.70−7.68 (m, 1 H), 7.60−7.54 (m, 2 H), 7.45−7.42 (m, 1 H), 7.34 (d, J = 8.1 Hz, 1 H), 7.24−7.20 (m, 1 H), 6.95 (d, J = 8.8 Hz, 1 H), 3.78 (s, 3H). ^{13}C NMR (D_2O, 100 MHz): 154.27, 139.79, 135.42, 127.07, 126.69, 125.60, 123.91, 121.70, 118.89, 113.17, 56.08. MS (ESI) calculated for $C_{15}H_{11}N_2NaO_6S$ $[(M - Na)]^-$, m/z 347.31, found $[(M - Na)]^-$, m/z 347.16.

(3fS). ^{1}H NMR (D_2O, 400 MHz): 7.90 (d, J = 0.9 Hz, 1 H), 7.65 (t, J = 1.3 Hz, 1 H), 7.63 (d, J = 1.3 Hz, 1 H), 7.36 (t, J = 7.2 Hz, 1 H), 7.04 (s, 2 H), 3.86 (s, 6 H). ^{13}C NMR (D_2O, 100 MHz): 154.24, 135.52, 132.18, 129.95, 127.47, 125.74, 119.42, 105.18, 56.44. MS (ESI) calculated for $C_{16}H_{13}N_2NaO_7S$ $[(M - Na)]^-$, m/z 377.34, found $[(M - Na)]^-$, m/z 377.17.

(3gS). ^{1}H NMR (D_2O, 400 MHz): 7.94 (s, 1 H), 7.79−7.72 (m, 2 H), 7.52−7.38 (m, 4 H). ^{13}C NMR (D_2O, 100 MHz): 154.18, 149.45, 135.61, 131.95, 127.73, 126.00, 125.85, 119.45, 116.27, 55.61, 42.50, 38.73. MS (ESI) calculated for $C_{14}H_8N_2Na_2O_9S_2$ $[(M - Na)]^-$, m/z 435.33, found $[(M - Na)]^-$, m/z 435.16.

(7S). ^{1}H NMR (D_2O, 400 MHz): 8.39−8.37 (m, 1 H), 8.33 (s, 1 H), 8.26 (t, J = 1.9 Hz, 1 H), 8.20 (t, J = 1.9 Hz, 1 H), 8.16−8.15 (m, 1 H), 8.02 (d, J = 8.1 Hz, 2H), 7.89−7.82 (m, 4 H), 7.55−7.50 (m, 3 H), 7.41−7.30 (m, 2 H), 7.24−7.21 (m, 1 H), 5.76 (s, 2 H), 4.61 (t, J = 6.4 Hz, 2 H), 4.64 (t, J = 6.9 Hz, 2 H), 2.25 (s, 3 H), 2.07−2.03 (m, 2 H), 1.84 (m, 2 H). ^{13}C NMR (D_2O, 100 MHz): 169.29, 166.11, 165.81, 158.70, 157.85, 153.85, 151.10, 150.82, 142.04, 138.84, 138.36, 134.40, 134.11, 129.69, 128.81, 127.58, 127.38, 126.98, 125.46, 124.80, 124.22, 123.27, 123.20, 123.16, 122.95, 121.29, 120.44, 114.51, 114.50. MS (ESI) calculated for $C_{37}H_{30}N_7NaO_8S$ $[(M - Na)]^-$, m/z 732.73, found $[(M - Na)]^-$, m/z 732.38.

(8S). ^{1}H NMR (D_2O, 400 MHz): 7.53−6.53 (m, 16 H), 5.11 (s, 2 H), 4.24 (s, 2 H), 3.62 (s, 2 H), 1.65 (s, 2 H), 1.26 (s, 2 H). ^{13}C NMR (D_2O, 100 MHz): 154.62, 151.52, 151.37, 151.02, 149.67, 149.38, 145.07, 142.68, 142.42, 138.21, 138.08, 136.39, 134.55, 133.70, 133.54, 130.28, 129.57, 127.21, 126.54, 126.31, 125.64, 125.31, 125.07, 124.33, 123.18, 122.26, 122.08, 121.17, 120.83, 119.94, 118.94, 113.42, 113.32, 65.92, 59.25, 55.53, 50.04, 39.56, 26.28, 25.00. MS (ESI) calculated for $C_{35}H_{27}N_7Na_2O_{10}S_2$ $[(M - Na)]^-$, m/z, 792.74, found $[(M - Na)]^-$, m/z 792.36.

(9S). ^{1}H NMR (D_2O, 400 MHz): 7.97 (s, 1 H), 7.87 (s, 1 H), 7.58−7.53 (m, 2 H), 7.24−6.99 (m, 9 H), 6.74−6.59 (m, 3 H), 5.25 (s, 2 H), 4.33 (t, J = 5.9 Hz, 2 H), 3.70−3.65 (m, 2 H), 2.23 (s, 3 H), 1.72 (s, 2 H), 1.32 (s, 2 H). ^{13}C NMR (100 MHz, D_2O): 172.29, 165.30, 165.09, 157.94, 157.09, 151.76, 151.51, 150.50, 149.65, 149.31, 142.83, 139.07, 138.07, 133.82, 129.67, 126.72, 125.74, 125,64, 125.30, 123.59, 122.46, 122.17, 120.87, 118.43, 118.24, 116.86, 113.57, 113.47, 65.96, 59.15, 55.49, 50.14, 26.23, 25.01, 20.54. MS (ESI) calculated for $C_{37}H_{29}N_7Na_2O_{12}S_2$ $[(M - Na)]^-$, m/z 850.78, found $[(M - Na)]^-$, m/z 850.39.

(10S). ^{1}H NMR (D_2O, 400 MHz): 7.86 (s, 1 H), 7.38−7.07 (m, 10 H), 6.86−6.70 (m, 3 H), 5.06 (s, 2 H), 4.35 (s, 2 H), 3.62 (d, J = 6.4 Hz, 6 H), 1.73 (s, 2 H), 1.36 (s, 2 H). ^{13}C NMR (D_2O, 100 MHz): 165.04, 164.63, 157.86, 157.63, 150.37, 150.31, 149.74, 149.40, 142.95, 142.28, 142.16, 134.29, 134.18, 133.67, 133.45, 126.16, 125.71, 125.56, 124.38, 122.40, 121.59, 120.91, 113.39, 113.31, 111.94, 55.67, 55.63, 50.09, 42.42, 26.23, 25.01. MS (ESI) calculated for $C_{37}H_{31}N_7Na_2O_{12}S_2$ $[(M - Na)]^-$, m/z, 852.79, found $[(M - Na)]^-$, m/z 852.40.

(11S). ^{1}H NMR (D_2O, 400 MHz): 8.11 (s, 1 H), 7.68 (s, 1 H), 7.59 (s, 1 H), 7.47−7.33 (m, 4 H), 7.27−7.19 (m, 3 H), 7.12−7.08 (m, 2 H), 7.03−6.99 (m, 3 H), 6.83−6.81 (m, 2 H), 5.25 (s, 2 H), 4.55 (t, J = 6.4 Hz, 2 H), 4.03 (t, J = 6.4 Hz, 2 H), 2.27−2.24 (m, 2 H). ^{13}C NMR (D_2O, 100 MHz): 167.17, 166.94, 160.26, 160.16, 158.53, 158.51, 152.81, 143.73, 140.30, 140.27, 134.74, 134.65, 130.27, 130.18, 128.70, 127.60, 127.48, 125.69, 124.31, 124.22, 120.64, 120.45, 118.57, 116.07, 115.99, 115.92, 115.87, 64.81, 60.94, 48.13, 30.01. MS (ESI) calculated for $C_{34}H_{25}N_7Na_2O_{10}S_2$ $[(M - Na)]^-$, m/z 778.71, found $[(M - Na)]^-$, m/z 778.11.

(12S). ^{1}H NMR (D_2O, 400 MHz): 7.96 (s, 1 H), 7.84(s, 1 H), 7.57(d, J = 8.5 Hz, 2 H), 7.44 (d, J = 7.2 Hz, 1 H), 7.17−6.9 (m, 9 H), 6.8−6.5 (m, 3 H), 5.24 (s, 2 H), 4.31 (s, 2 H), 3.6 (s, 2 H), 1.69 (s, 2 H), 1.28 (s, 2 H). ^{13}C NMR (D_2O, 100 MHz): 165.27, 158.43, 157.87, 153.18, 151.46, 149.68, 149.43, 142.81, 138.07, 133.99, 129.51, 126.61, 125.61, 125.45, 125.17, 123.55, 120.86, 113.19, 65.89, 50.15, 42.43, 26.12, 24.91. ESI-TOF (HRMS) calculated for $C_{35}H_{27}N_7Na_2O_{10}S_2$ $[(M - Na)]^-$, m/z 792.1164, found $[(M - Na)]^-$, m/z 792.1194 and $[(M - 2Na)]^{2-}$, m/z 384.5643.

(13S). ^{1}H NMR (D_2O, 400 MHz): 7.79−7.75 (m, 3 H), 7.61(d, J = 7.8 Hz, 2 H), 7.17−7.02 (m, 9 H), 6.81−6.69 (m, 3 H), 5.13 (s, 2H), 4.25 (s, 2 H), 3.61 (s, 2 H), 1.65 (s, 2 H), 1.27 (s, 2 H). ^{13}C NMR (D_2O, 100 MHz): 165.41, 164.97, 158.34, 158.12, 153.52, 153.46, 149.64, 149.1, 142.82, 133.85, 133.62, 133.52, 129.57, 126.55, 126.40, 125.25, 124.78, 122.47, 120.93, 120.86, 113.38, 113.25, 65.97, 52.1, 50.07, 26.12, 24.91. ESI-TOF (HRMS) calculated for $C_{35}H_{27}N_7Na_2O_{10}S_2$ $[(M - Na)]^-$, m/z 792.1164, found $[(M - Na)]^-$, m/z 792.1172 and $[(M - 2Na)]^{2-}$, m/z 384.5628.

(14S). ^{1}H NMR (D_2O, 400 MHz): 7.84 (s, 1 H), 7.78 (d, J = 8.6 Hz, 2 H), 7.60(s, 1 H), 7.40 (d, J = 7.6 Hz, 2 H), 7.22−6.99 (m, 8 H), 6.78 (d, J = 7.8 Hz, 1 H), 6.68−6.66 (m, 2 H), 5.15 (s, 2 H), 4.27 (s, 2 H), 3.65 (s, 2 H), 1.68 (s, 2 H), 1.30 (s, 2 H). ^{13}C NMR (D_2O, 100 MHz): 165.40, 158.44, 153.90, 151.74, 149.35, 143.14, 138.08, 134.1, 133.73, 129.86, 126.85, 125.65, 125.06, 123.73, 122.72, 121.19, 121.01, 113.66, 66.33, 59.61, 50.33, 26.36, 25.24. MS (ESI) calculated for $C_{35}H_{27}N_7Na_2O_{10}S_2$ $[(M - Na)]^-$, m/z 792.76, found $[(M - Na)]^-$, m/z 792.14.

(15S). ^{1}H NMR (D_2O, 400 MHz): 7.85 (d, J = 8.7 Hz, 2 H), 7.78 (s, 1 H), 7.65 (d, J = 8.6 Hz, 2 H) 7.23−7.05 (m, 9 H), 6.97−6.94 (m, 1 H), 6.38−6.72 (m, 2 H), 5.19 (s, 2 H), 4.27 (s, 2 H), 3.57 (s, 2 H), 1.68 (s, 2 H), 1.21 (s, 2 H), 0.95 (s, 2 H). ^{13}C NMR (D_2O, 100 MHz): 165.06, 158.48, 158.27, 153.49, 153.36, 149.79, 149.42, 142.84, 133.85, 129.63, 129.53, 126.55, 125.59, 122.45, 121.0, 120.79, 113.45, 112.38, 66.33, 58.85, 50.23, 28.92, 27.05, 22.31. ESI-TOF (HRMS) calculated for $C_{36}H_{29}N_7Na_2O_{10}S_2$ $[(M - Na)]^-$, m/z 806.1321, found $[(M - Na)]^-$, m/z 806.1327 and $[(M - 2Na)]^{2-}$, m/z 391.5690.

(16S). ^{1}H NMR (D_2O, 400 MHz): 7.89 (d, J = 8.6 Hz, 2 H), 7.73−7.69 (m, 3 H), 7.23−7.10 (m, 9 H), 6.96−6.94 (m, 1 H), 6.77−6.69 (m, 2 H), 5.15 (s, 2 H), 4.16 (s, 2 H), 3.57 (s, 2 H), 1.50 (s, 2 H), 1.02 (s, 2 H), 0.80 (s, 4 H). ^{13}C NMR (D_2O, 100 MHz): 158.57, 158.40, 153.54, 149.92, 149.70, 142.78, 133.99, 129.67, 129.52, 126.26, 125.74, 122.37, 121.0, 120.81, 113.54, 66.37, 55.49, 42.41, 29.33, 25.55, 24.75, 12.32. ESI-TOF (HRMS) calculated for $C_{37}H_{31}N_7Na_2O_{10}S_2$ $[(M - Na)]^-$, m/z 820.1477, found $[(M - Na)]^-$, m/z 820.1467 and $[(M - 2Na)]^{2-}$, m/z 398.5775.

(17S). ^{1}H NMR (D_2O, 400 MHz): 8.17 (s, 1 H), 7.87 (s, 1 H), 7.34−7.13(m, 10 H), 6.96−6.87 (m, 2 H), 6.68−6.57 (m, 3 H), 5.38 (s, 2 H), 4.24 (s, 2 H), 3.74 (s, 2 H), 3.64 (s, 3 H), 1.81 (s, 2 H), 1.43 (s, 2 H). ^{13}C NMR (D_2O, 100 MHz): 165.40, 158.05, 157.44, 153.43,

dx.doi.org/10.1021/jm301757v | J. Med. Chem. XXXX, XXX, XXX−XXX

151.25, 148.62, 142.76, 139.62, 134.24, 133.92, 129.63, 126.66, 126.39, 125.95, 125.32, 123.47, 122.83, 122.24, 122.06, 120.73, 113.27, 112.38, 66.33, 55.85, 50.27, 26.13, 24.98. MS (ESI) calculated for $C_{36}H_{29}N_7Na_2O_{11}S_2$ $[(M - Na)]^-$, m/z 822.79, found $[(M - Na)]^-$, m/z 822.16.

(18S). ^{1}H NMR (D_2O, 400 MHz): 8.52−8.50 (m, 2 H), 8.33−8.31 (m, 3 H), 8.02−7.97 (m, 2 H), 7.83−7.77 (m, 4 H), 7.48−7.44 (m, 5 H), 5.77 (s, 2 H), 4.62−4.57 (m, 4 H), 2.20−2.14 (m, 2 H), 1.96−1.91 (m, 2 H). ^{13}C NMR(D_2O, 100 MHz): 167.93, 167.39, 160.51, 159.86, 156.45, 154.71, 152.91, 152.73, 144.29, 141.07, 135.32, 135.23, 135.12, 10.83, 128.62, 128.35, 128.02, 126.18, 124.58, 124.53, 122.06, 118.89, 118.09, 116.27, 115.90, 67.63, 61.01, 28.13, 26.93. MS (ESI) calculated for $C_{35}H_{26}N_7Na_3O_{14}S_3$ $[(M - Na)]^-$, m/z 910.78, found m/z 910.33.

(19S). ^{1}H NMR (CD_3OD, 400 MHz): 8.62 (s, 1 H), 8.45 (d, J = 2.1 Hz, 2 H), 8.34 (t, J = 1.5 Hz, 1 H), 8.14−8.04 (m, 3 H), 7.92−7.82 (m, 4 H), 7.57 (m, 2 H), 7.38 (t, J = 2.1 Hz, 1 H), 7.25 (t, J = 2.1 Hz, 1 H), 5.84 (s, 2 H), 4.66−4.58 (m, 4 H), 2.33 (s, 3 H), 2.22−2.17 (m, 2 H), 1.95−1.91 (m, 2 H). ^{13}C NMR (CD_3OD, 100 MHz): 171.02, 168.11, 167.48, 159.77, 159.72, 154.78, 152.97, 152.70, 141.29, 140.82, 135.22, 135.11, 128.72, 128.57, 128.38, 128.30, 124.68, 124.54, 119.83, 119.11, 118.59, 118.28, 118.02, 116.42, 116.37, 67.66, 28.11, 26.86, 21.0. MS (ESI) calculated for $C_{37}H_{28}N_7Na_3O_{16}S_3$ $[(M - 2SO_3 - Na)]^-$, m/z 764.80, found $[(M - 2SO_3 - Na)]^-$, m/z 764.37.

(20S). ^{1}H NMR (D_2O, 400 MHz): 8.61 (s, 1 H), 7.35−7.09 (m, 11 H), 6.80−6.70 (m, 3 H), 5.87 (s, 2 H), 4.72 (s, 2 H), 4.61 (s, 2 H), 2.25−2.21 (m, 2 H), 1.99−1.93 (m, 2 H). ^{13}C NMR (D_2O, 100 MHz): 168.12, 167.53, 160.10, 159.82, 154.84, 154.64, 153.03, 152.85, 143.93, 141.06, 140.84, 135.28, 135.10, 128.77, 128.63, 128.36, 128.32, 127.18, 124.60, 118.96, 118.54, 118.19, 118.00, 116.42, 116.40, 67.71, 60.67, 28.24, 26.93, 24.99. MS (ESI) calculated for $C_{35}H_{25}N_7Na_4O_{18}S_4$ $[(M - 3SO_3 - Na^+)]^-$, m/z 719.83, found $[(M - 3SO_3 - Na^+)]^-$, m/z 722.30.

(25S). ^{1}H NMR (D_2O, 400 MHz): 8.12 (s, 1 H), 7.82−7.16 (m, 10 H), 6.48 (d, J = 2.1 Hz, 1 H), 6.36 (d, J = 2.1 Hz, 1 H), 5.47 (s, 2H), 4.56 (t, J = 6.1 Hz, 2 H), 4.12 (t, J = 6.4 Hz, 2 H), 3.59 (s, 3 H), 2.0−1.9 (m, 2 H), 1.68−1.61 (m, 2 H). ^{13}C NMR (D_2O, 100 MHz): 173.48, 159.61, 156.42, 156.11, 154.9, 151.38, 149.79, 148.65, 143.65, 143.33, 138.44, 134.38, 133.46, 129.87, 127.24, 127.14, 125.87, 125.79, 125.02, 123.73, 123.11, 122.55, 121.14, 116.09, 113.66, 110.12, 101.10, 100.42, 66.47, 62.52, 56.04, 50.46, 26.19, 25.03. MS (ESI) calculated for $C_{37}H_{27}N_5Na_4O_{21}S_4$ $[(M - 3Na)]^-$, m/z 1028.89, found $[(M - 3Na)]^-$, m/z 1028.82.

(26S). ^{1}H NMR (D_2O, 400 MHz): 8.15 (s, 1 H), 7.57−7.05 (m, 10 H), 6.51 (d, J = 2.1 Hz, 1 H), 6.36 (d, J = 2.1 Hz, 1 H), 5.48 (s, 2 H), 4.56 (t, J = 6.2 Hz, 2 H), 4.12 (t, J = 6.4 Hz, 2 H), 3.49 (s, 3 H), 3.42 (s, 3 H), 2.04−1.98 (m, 2 H), 1.89−1.71 (m, 2 H). ^{13}C NMR (D_2O, 100 MHz): 173.48, 159.61, 156.42, 156.11, 154.9, 151.38, 149.79, 148.65, 143.65, 143.33, 138.44, 134.38, 133.46, 129.87, 127.24, 127.14, 125.87, 125.79, 125.02, 123.73, 123.11, 122.55, 121.14, 116.09, 113.66, 110.12, 101.10, 100.42, 66.47, 62.52, 56.04, 50.46, 26.19, 25.03. MS (ESI) calculated for $C_{38}H_{29}N_5Na_4O_{22}S_4$ $[(M - 3Na)]^-$, m/z 1058.88, found $[(M - 3Na)]^-$, m/z 1058.90 $[(M + Na)]^-$.

(27S). ^{1}H NMR (D_2O, 400 MHz): 8.12 (s, 1 H), 7.75−7.14 (m, 10 H), 6.52−6.51 (m, 1 H), 6.30−6.28 (m, 1 H), 5.46 (s, 2 H), 4.56−4.53 (m, 2 H), 4.09−4.06 (m, 2 H), 3.5 (s, 2 H), 2.39 (s, 3 H), 2.01−2.0 (m, 2 H), 1.60−1.59 (m, 2 H). ^{13}C NMR (D_2O, 100 MHz): 173.31, 172.72, 159.53, 156.41, 156.18, 154.88, 151.81, 150.74, 148.60, 143.57, 143.38, 139.38, 134.47, 133.38, 127.42, 127.29, 126.04, 124.99, 123.22, 122.52, 119.00, 118.79, 117.35, 116.09, 113.79, 109.98, 100.89, 100.38, 66.49, 62.49, 55.98, 50.44, 26.24, 25.01, 20.64. MS (ESI) calculated for$C_{39}H_{29}N_5Na_4O_{23}S_4$ $[(M - 3Na)]^-$, m/z 1086.93, found $[(M - 3Na)]^-$, m/z 1086.90.

(28S). ^{1}H NMR (D_2O, 400 MHz): 7.76 (d, J = 8.12 Hz, 4 H), 7.28−7.18 (m, 6 H), 7.05−6.91 (m, 6 H), 6.80−6.77 (m, 2 H), 4.92 (s, 4 H), 4.87 (s, 4 H). ^{13}C NMR (D_2O, 100 MHz): 164.76, 158.22, 153.35, 149.42, 142.91, 133.90, 133.82, 129.71, 126.67, 125.32, 125.22, 120.98, 112.88, 59.43, 49.90. ESI-TOF (HRMS) calculated for $C_{36}H_{26}N_{10}Na_2O_{10}S_2$ $[(M - Na)]^-$, m/z 845.1178, found $[(M - Na)]^-$, m/z 845.1142 and $[(M - 2Na)]^{2-}$, m/z 411.0621.

(29S). ^{1}H NMR (D_2O, 400 MHz): 7.88 (d, J = 8.6 Hz, 2 H), 7.74−7.67 (m, 3 H), 7.26−7.07 (m, 7 H), 6.94−6.90 (m, 2 H), 6.64−6.62 (m, 3 H), 5.22 (s, 2 H), 4.21 (s, 2 H), 3.50 (s, 2 H), 1.66 (s, 2 H), 1.16 (s, 2 H), 0.91 (s, 2 H). ^{13}C NMR (D_2O, 100 MHz): 165.28, 158.55, 158.11, 153.59, 153.42, 149.59, 134.11, 133.69, 129.70, 129.58, 126.41, 122.00, 121.07, 120.95, 113.28, 113.16, 65.73, 48.20, 42.41, 28.94, 22.10, 12.34. ESI-TOF (HRMS) calculated for $C_{36}H_{29}N_7Na_2O_{10}S_2$ $[(M - Na)]^-$, m/z 806.1321, found $[(M - Na)]^-$, m/z 806.1316 and $[(M - 2Na)]^{2-}$, m/z 391.5695.

Direct Inhibition of Factor XIa by Sulfated QAOs. A chromogenic substrate hydrolysis assay using a microplate reader (FlexStation III, Molecular Devices) was used to measure direct inhibition of FXIa, as described earlier.[31] Generally, each well of the 96-well microplate had 85 μL of pH 7.4 buffer (50 mM Tris−HCl, 150 mM NaCl, 0.1% PEG8000, and 0.02% Tween80) to which 5 μL of a potential FXIa inhibitor (or solvent reference) was added followed by 5 μL of FXIa to give 0.765 nM in the well. After 10 min incubation at 37 °C, 5 μL of FXIa substrate S2366 (345 μM in the well) was rapidly added, and the residual FXIa activity was measured from the initial rate of increase in absorbance at 405 nm. Stocks of FXIa inhibitors were 20 mM, which were then serially diluted to give 12 different aliquots in the plate wells. Relative residual FXIa activity at each concentration of the inhibitor was calculated from the ratio of FXIa activity in the presence and absence of the inhibitor. Logistic eq 1 was used to fit the dose dependence of the residual proteinases activity to obtain the potency (IC_{50}) and efficacy (ΔY) of inhibition. In this equation, Y is the ratio of residual factor XIa activity in the presence of inhibitor to that in its absence (fractional residual activity), Y_M and Y_0 are the maximum and minimum possible values of the fractional residual proteinase activity, IC_{50} is the concentration of the inhibitor that results in 50% inhibition of enzyme activity, and HS is the Hill slope. Nonlinear curve fitting resulted in Y_M, Y_0, IC_{50} and HS values:

$$Y = Y_0 + \frac{Y_M - Y_0}{1 + 10^{(\log[I]_0 - \log IC_{50}) \times HS}} \quad (1)$$

Inhibition of Other Proteases of the Coagulation and Digestive Systems. The inhibition potential of 500 μM SAM (**16S**, **15S**, **13S**) against coagulation enzymes including thrombin and factor Xa and digestive enzymes including trypsin and chymotrypsin was evaluated using chromogenic substrate hydrolysis assays reported in the literature.[26,28,31] These assays were performed using substrates appropriate for the enzyme being studied under conditions closest to the physiological condition (37 °C and pH 7.4), except for thrombin, which was performed at 25 °C and pH 7.4. The concentrations of enzymes and substrates in microplate wells, respectively, were as follows: 6 nM and 50 μM for thrombin; 1.09 nM and 125 μM for factor Xa; 2.5 ng/mL and 80 μM for bovine trypsin; and 500 ng/mL and 240 μM for bovine chymotrypsin. The ratio of the proteolytic activity of an enzyme in the presence of the sulfated QAO to that in its absence was used to calculate percent inhibition (%).

Michaelis−Menten Kinetics of Substrate Hydrolysis in Presence of 14S. The initial rate of S2366 hydrolysis by FXIa was obtained from the linear increase in absorbance at 405 nm corresponding to less than 10% consumption of S2366. The initial rate was measured as a function of various concentrations of the substrate (0.01−1.6 mM) in the presence of fixed concentration of **14S** in 50 mM Tris−HCl buffer, pH 7.4, containing 150 mM NaCl, 0.1% PEG8000, and 0.02% Tween80 at 37 °C. The data was fitted using the standard Michaelis−Menten eq 2 to determine the K_M and V_{max}:

$$V_i = \frac{V_{max}[S]}{K_M + [S]} \quad (2)$$

Thermodynamics of Sulfated QAOs Binding to Human Factor XIa. Fluorescence experiments were performed using a QM4 spectrofluorometer (Photon Technology International, Birmingham, NJ) in 50 mM Tris−HCl buffer of pH 7.4 containing 150 mM NaCl and 0.1% PEG8000 at 37 °C. Fluorescence emission spectra of active-site labeled FXIa, that is, FXIa-DEGR (250 nM), in the absence and

dx.doi.org/10.1021/jm301757v | J. Med. Chem. XXXX, XXX, XXX−XXX

Scheme 1. Synthesis of Monomeric Sulfated QAOs[a]

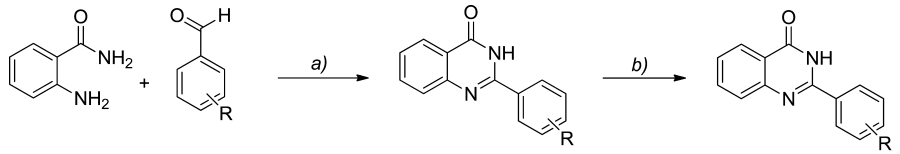

[a]Conditions: (a) $NaHSO_3$, DMA, reflux/overnight, 65−80%; (b) SO_3/Me_3N, TEA, CH_3CN, microwave/30 min, 85−90%.

presence of saturating concentrations of sulfated QAOs (**13S**−**16S**) were recorded using an excitation wavelength of 345 nm. The emission scan range was set to 350−600 nm in increments of 1 nm. The excitation and emission slit widths were set at 1 mm and 1.5 mm, respectively. The equilibrium dissociation constant (K_D) of the sulfated QAOs−FXIa complex was measured using the change in the fluorescence of the active site dansyl group due to binding. Titrations were performed by adding aliquots of a solution of sulfated QAOs (**13S**−**16S**) in the above buffer to a fixed concentration of FXIa-DEGR (250 nM) and monitoring the change in the fluorescence of FXIa-DEGR at 547 nm (λ_{ex} = 345 nm). The slit widths on the excitation and emission side were 1 and 1.5 mm, respectively. The change in fluorescence at 547 nm was fitted using the standard Hill equation for ligand binding (eq 3) for cooperative binding to obtain the apparent dissociation constant ($K_{D,app}$) of binding. In this equation, ΔF represents the change in fluorescence following addition of the sulfated QAO from the initial fluorescence (F_0), while ΔF_{max} represents the maximal change in fluorescence. The Hill coefficient "n" is a measure of the cooperativity of binding. Each measurement was performed at least twice:

$$\frac{\Delta F}{F_0} = \Delta F_{max} \times \frac{[\text{sulfated QAO}]^n}{(K_{D,app})^n + [\text{sulfated QAO}]^n} \quad (3)$$

Prothrombin Time (PT) and Activated Partial Thromboplastin Time (APTT). Clotting time was measured in a standard one-stage recalcification assay with a BBL Fibrosystem fibrometer (Becton−Dickinson, Sparles, MD). For PT assays, thromboplastin-D was reconstituted according to the manufacturer's directions and warmed to 37 °C. A 10 μL amount of sulfated quinazolinones (**13S**, **15S**, and **16S**), to give the desired concentration, was brought up to 100 μL with citrated human plasma, incubated for 30 s at 37 °C followed by addition of 200 μL of prewarmed thromboplastin-D. For the APTT assay, 10 μL of the same molecules was mixed with 90 μL of citrated human plasma and 100 μL of prewarmed APTT reagent (0.2% ellagic acid). After incubation for 4 min at 37 °C, clotting was initiated by adding 100 μL of prewarmed 25 mM $CaCl_2$, and the time to clot was noted. The data were fit to a quadratic trend line, which was used to determine the concentration of the inhibitor necessary to double the clotting time. Clotting time in the absence of an anticoagulant was determined in a similar fashion using 10 μL of deionized water and/or the appropriate organic vehicle and was found to be 17.6 s for PT and 39.9 s for APTT.

Mutagenesis and Expression of Recombinant Factor XIa. Mutations in the FXIa 170 helix were introduced into a modified human FXI cDNA (FXI-Ser-362,482), which contains serine substitutions for Cys362 and Cys482 (FXI numbering), as described earlier in several papers.[32,33] A disulfide bond between these residues connects the heavy chains and catalytic domains after cleavage at the activation site, and eliminating the bond allows the catalytic domain of FXIa (FXIa-CD) to separate from the heavy chain. The basic residues of the FXIa 170-helix, Lys529, Arg530, Arg532, Lys535 and Lys539 in the FXI numbering system (corresponding to residues 170, 171, 173, 175, and 179 in the chymotrypsinogen numbering system), were changed to alanine individually and as a group using a Quick Change kit (Stratagene, La Jolla, CA). cDNAs in expression vector pJVCMV were used to transfect HEK-293 cells as described. Stably expressing clones were expanded in 175 cm^2 flasks, and serum-free media (Cellgro Complete, Mediatech, Herndon, VA) was collected every 48 h, supplemented with benzamidine (5 mM) and stored at −80 °C pending purification. Recombinant FXI was purified from conditioned media on an anti-fXI IgG 1G5.12 affinity column. After loading, the column was washed with 25 mM Tris−HCl, pH 7.4, 100 mM NaCl, and eluted with 2 M NaSCN in the same buffer. Protein containing fractions were pooled, concentrated, and dialyzed, and protein concentrations were determined by dye-binding assay (Bio-Rad). Recombinant wild-type FXI or FXI-CD (~200−300 μg/mL) was activated with 5 μg/mL FXIIa at 37 °C. Completion of activation was confirmed by sodium dodecyl sulfate polyacrylamide gel electrophoresis (SDS-PAGE). Activated preparations were passed over a 1G5.12 column to separate the protease from FXIIa. In the case of proteins prepared in FXI-Ser-362,482, the catalytic domains bind to the column, while the heavy chain passes through.

RESULTS AND DISCUSSION

Synthesis of the Library of QAOs. To put the dual element hypothesis of Figure 1 to test, we synthesized a library of 26 QAOs including 7 monomers and 19 dimers containing 1−4 sulfate groups. The QAO core structure is a well-known hP scaffold with three-dimensional similarity to the flavonoid scaffold studied earlier as a HBS ligand.[18−22] The QAO core scaffold was synthesized using a condensation reaction between anthranilamide and suitably substituted benzaldehyde[34] to obtain QAO monomers **3a**−**3g** containing one or two phenolic groups (Scheme 1). This is a fairly well-established thermal cyclodehydration reaction. Yet, the reaction yields decrease as the number of phenolic groups increase restricting the library diversity to two phenolic groups on the scaffold. Monomers **3a**−**3g** were sulfated under microwave conditions[29,30] to yield the corresponding sulfated derivatives **3aS**−**3gS** in 85−90% yields. Sulfation changes the physicochemical characteristics of the QAO scaffold by introducing significant water solubility. Water-soluble sulfated molecules have been previously purified using size-exclusion chromatography.[29,30] However, the considerable hydrophobicity of the QAO scaffold allowed for the use of a traditional dichloromethane−methanol solvent system using flash chromatography. This greatly eased handling of these highly polar compounds. The sulfated QAOs were characterized using ^1H and ^{13}C NMR and ESI-MS techniques.

To develop a more diverse library, dimerization of the monomeric scaffold was desirable. A rather simple tool for generating a dimeric equivalent is the copper-catalyzed azide−

dx.doi.org/10.1021/jm301757v | J. Med. Chem. XXXX, XXX, XXX−XXX

Scheme 2. Synthesis of Sulfated QAOs 7S−20S[a]

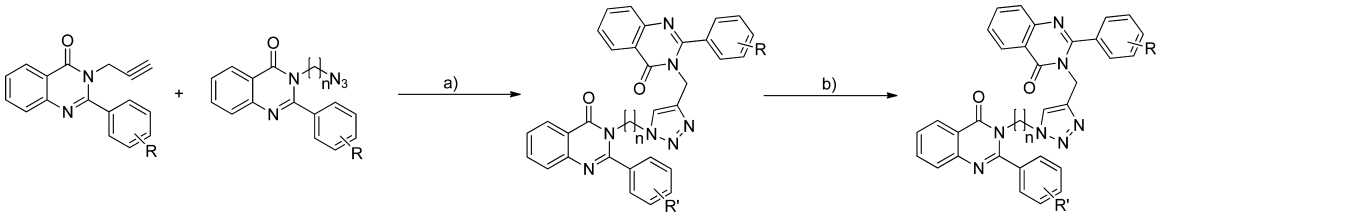

4a: R = 3 OAc
5a: R = 3-OH
5b: R = 4-OH
5c: R = 3, 5-OH
5d: R = 3-OMe, 4-OH

6a: R = 3-OH, n = 4
6b: R = 4-OH, n = 4
6c: R = 3, 5-OH, n = 4
6d: R = 3-OMe, 4-OH, n = 4
6e : R = 3-OH, n = 3
6f : R = 4-OH, n = 5
6g: R = 4-OH, n =6
6h: R = 3-OAc, 5-OH, n = 4

7 : R = 3-OAc, R' = 3-OH, n = 4
8 : R = 3-OH, R' = 3-OH, n = 4
9 : R = 3-OH, 5-OH, R' = 3-OAc n = 4
10 : R = 3-OMe, 4-OH, R' = 3-OMe, 4-OH, n = 4
11 : R = 3-OH, R' = 3-OH, n = 3
12 : R = 3-OH, R' = 4-OH, n = 4
13 : R = 4-OH, R' = 4-OH, n = 4
14 : R = 4-OH, R' = 3-OH, n = 4
15 : R = 4-OH, R' = 4-OH, n = 5
16 : R = 4-OH, R' = 4-OH, n = 6
17 : R = 3-OH, R' = 3-OMe, 4-OH, n = 4
18 : R = 3-OH, 5-OH, R' = 3-OH, n = 4
19 : R = 3-OH, 5-OH, R' = 3-OAc, 5-OH, n = 4
20 : R = 3-OH, 5-OH, R' = 3-OH, 5-OH, n = 4

7S : R = 3 -OAc, R' = 3-OSO_3^-, n = 4
8S : R = 3-OSO_3^-, R' = 3-OSO_3^-, n = 4
9S : R = 3-OSO_3^-, 5-OSO_3^-, R' = 3-OAc, n = 4
10S : R = 3-OMe, 4-OSO_3^-, R' = 3-OMe, 4-OSO_3^-, n = 4
11S : R = 3-OSO_3^-, R' = 3-OSO_3^-, n = 3
12S : R = 3-OSO_3^-, R' = 4-OSO_3^-, n = 4
13S : R = 4-OSO_3^-, R' = 4-OSO_3^-, n = 4
14S : R = 4-OSO_3^-, R' = 3-OSO_3^-, n = 4
15S : R = 4-OSO_3^-, R' = 4-OSO_3^-, n = 5
16S : R = 4-OSO_3^-, R' = 4-OSO_3^-, n = 6
17S : R = 3-OSO_3^-, R' = 3-OMe, 4-OSO_3^-, n = 4
18S : R = 3-OSO_3^-, 5-OSO_3^-, R' = 3-OSO_3^-, n = 4
19S : R = 3-OSO_3^-, 5-OSO_3^-, R' = 3-OAc, 5-OSO_3^- , n = 4
20S : R = 3-OSO_3^-, 5-OSO_3^-, R' = 3-OSO_3^-, 5-OSO_3^-, n = 4

[a]Conditions: (a) $CuSO_4 \cdot 5H_2O$ (1 mol %), sodium ascorbate (5 mol %), DMF/H_2O (1:1), room temperature (rt)/overnight, 80−95%; (b) SO_3/Me_3N, TEA, CH_3CN, microwave/30 min, 85−90%.

Scheme 3. Synthesis of Sulfated QAOs 25S−27S[a]

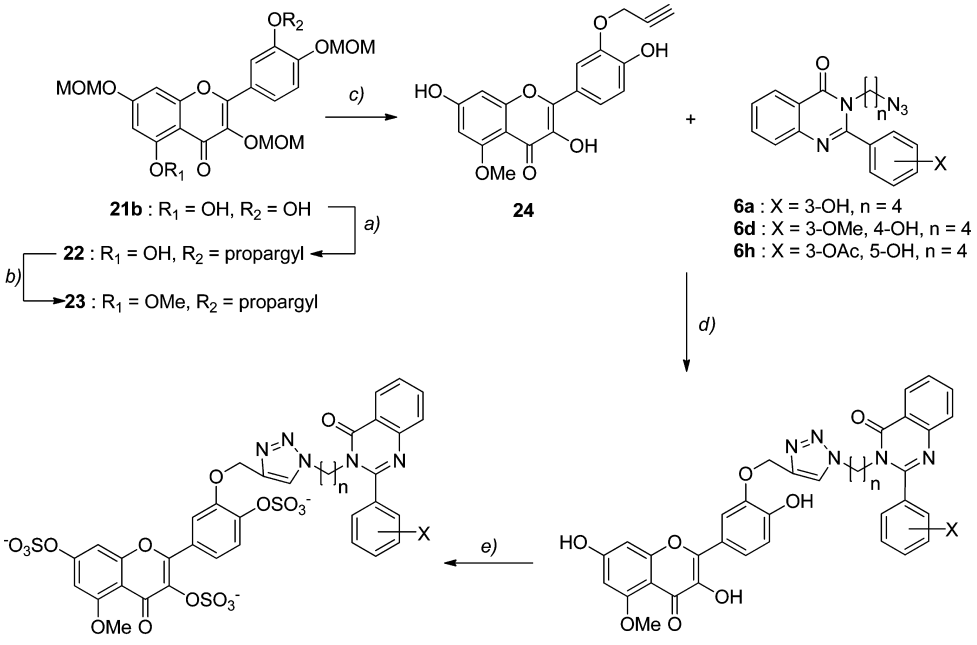

21b : R_1 = OH, R_2 = OH
22 : R_1 = OH, R_2 = propargyl
23 : R_1 = OMe, R_2 = propargyl

24

6a : X = 3-OH, n = 4
6d : X = 3-OMe, 4-OH, n = 4
6h : X = 3-OAc, 5-OH, n = 4

25S : X = 3-OSO_3^-, n = 4
26S : X = 3-OMe, 4-OSO_3^-, n = 4
27S : X = 3-OAc, 5--OSO_3^-, n = 4

25 : X = 3-OH, n = 4
26 : X = 3-OMe, 4-OH, n = 4
27 : X = 3-OAc, 5-OH, n = 4

[a]Conditions: (a) K_2CO_3, propargyl bromide, DMF, rt/2 h, 85−90%; (b) K_2CO_3, MeI, DMF, rt/4 h, 85−90%; (c) 3N HCl, acetone, reflux/overnight, 55−60%; (d) $CuSO_4 \cdot 5H_2O$ (1 mol %), sodium ascorbate (5 mol %), DMF/H_2O (1:1), rt/overnight, 80−95%; (e) SO_3/Me_3N, Et_3N, CH_3CN, microwave/30 min, 85−90%.

alkyne cycloaddition (CuAAC) reaction.[35] Thus, QAO alkynes **4a−5d** and azides **6a−6h** (Scheme 2) were synthesized from corresponding monomers **3a−3d** using acetylation of phenolic group followed by standard nucleophilic displacement strategy and and deacetylation in excellent yields (see the Supporting Information). Varying the linker length (n = 3−6) in the azide **6** scaffold afforded an opportunity of expanding the diversity of the library. CuAAC in the presence of aqueous $CuSO_4$ (1 mol %) and sodium ascorbate (5 mol %) gave 1,2,3-triazoles **7−20** (Scheme 2). The high reaction yields (80−95%) observed for the QAO series coupled with an essentially single product suggested 1,4-substitution of the triazole, as established in the literature.[35] Intermediates **7−20** were sulfated using the microwave conditions developed for monomers to obtain sulfated QAOs **7S−20S** (Scheme 2). The reaction resulted in sulfation of each available −OH group to give a single

dx.doi.org/10.1021/jm301757v | J. Med. Chem. XXXX, XXX, XXX−XXX

Scheme 4. Synthesis of Sulfated QAO 28S[a]

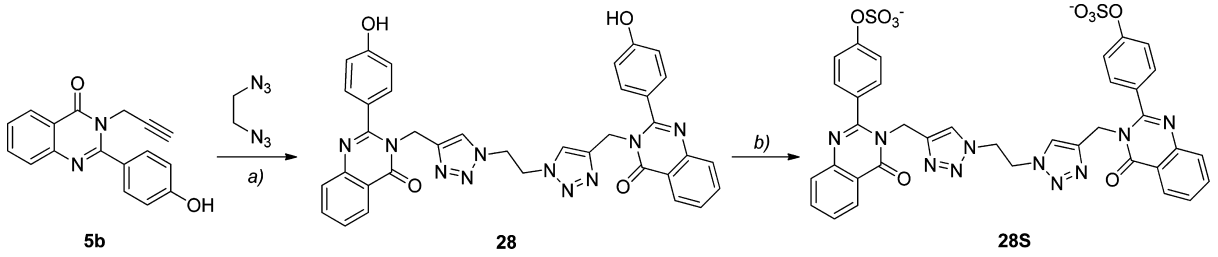

[a]Conditions: (a) $CuSO_4 \cdot 5H_2O$ (2 mol %), sodium ascorbate (10 mol %), DMF/H_2O (1:1), rt/overnight, 80%; (b) SO_3/Me_3N, Et_3N, CH_3CN, microwave/30 min, 90%.

Scheme 5. Synthesis of Sulfated QAO 29S[a]

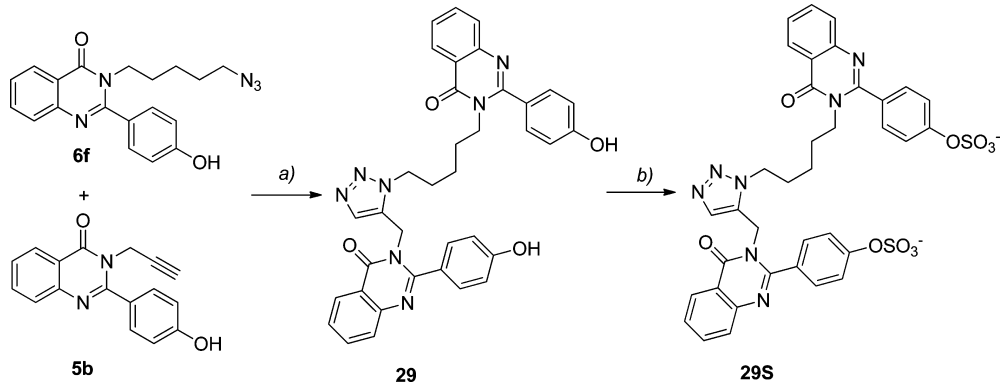

[a]Conditions: (a) $CpRuCl(PPh_3)_2$, dioxane, 60 °C/overnight, 80%; (b) SO_3/Me_3N, Et_3N, CH_3CN, microwave/30 min, 90%.

persulfated product, which simplified purification resulting in 80−90% yields.

Compounds **7S−20S** contain an identical QAO unit at either end and will be referred to herein as homo-"click" dimers, although these are not truly symmetric. To explore further structural dependence, inhibitors **25S−27S** were synthesized (Scheme 3). These contain a flavonoid core on one end and a QAO core on the other (hetero-"click" dimers). The major structural difference between the two types of click dimers is the higher sulfation level of the flavonoid scaffold. Utilizing an intramolecular H-bond-dependent protection−deprotection strategy, flavonoid **21b** was transformed into propargyl derivative **24**, which gave **25−27** upon CuAAC with azides **6a**, **6d**, and **6h** (Scheme 3). Sulfation of these molecules resulted in flavonoid−QAO hetero-click dimers **25S−27S**.

To study the dependence of inhibition on the geometry of the linker, a double-click sulfated QAO dimer **28S** was synthesized using a slight modification of the strategy developed for homo-click dimers (Scheme 4). Inhibitor **28S** contains two 1,4-triazole units, instead of one 1,4-triazole moiety in **7S−21S** and **25S−27S**. Finally, geometric isomerism in the linker was also studied. Whereas all click dimers contained a 1,4-substituted triazole moiety, **29S** contained a 1,5-substituted triazole moiety. Inhibitor **29S** was synthesized from phenolic precursor **29**, which was synthesized in high yields using a ruthenium-catalyzed cycloaddition[36] of azide **6f** and alkyne **5B** (Scheme 5). Comparison of ^1H NMR spectra of regioisomers **15** and **29** shows that the methylenic protons attached to the triazole moiety in each case was significantly different. Whereas 1,4-substituted triazole **15** showed the $C\underline{H}_2$ at 5.81 δ, **29** displays the corresponding signal at 5.96 δ confirming the difference in geometries.

In combination, the library of 26 sulfated QAOs was synthesized through the use of simple synthetic tools in generally high yields. Structural diversity in this family of sulfated hydrophobic small molecules arises from the number of sulfate groups on the core scaffold (1−4), the position of sulfate groups (either 2, 3, 4, or 5 on the aromatic ring), the type of core scaffolds (QAO or flavonoid), the type of linker (1 or 2 triazoles), the length of linker (8−11 intervening atoms), and the geometry of the linker (1,4- or 1,5-triazole). This is a first small library of potential GAG mimetics that is based on a fully synthetic, heterocyclic scaffold. The success of this synthetic venture indicates the feasibility of the development of other novel GAG mimetics based on a sulfated hydrophobic scaffold.

Inhibition of Human Factor XIa by Sulfated QAOs. The library of sulfated QAOs was screened for inhibition of human FXIa and other coagulation enzymes using chromogenic substrate hydrolysis assay, as described earlier.[22,28,31] The sigmoidal decrease in the initial rate of protease activity (on a semilog plot) as a function of ligand concentration was fitted using the logistic dose−response equation to calculate the IC_{50}. Of the 26 sulfated QAOs studied, 16 exhibited inhibition of factor XIa at pH 7.4 and 37 °C (Figure 2A) suggesting a good "hit" ratio arising from the novel SAM discovery strategy. Most importantly, the unsulfated precursors of the 26 sulfated molecules did not inhibit factor XIa at all highlighting the importance of the anionic group (—OSO_3^-) as a recognition element.

The range of inhibitory potency was found to be reasonable (50 to >1000 μM), while the efficacy for nearly all inhibitors was very high (>85%). Inhibitor **26S** displayed an efficacy of approximately 50%, which supports the possibility of structure-

dx.doi.org/10.1021/jm301757v | J. Med. Chem. XXXX, XXX, XXX−XXX

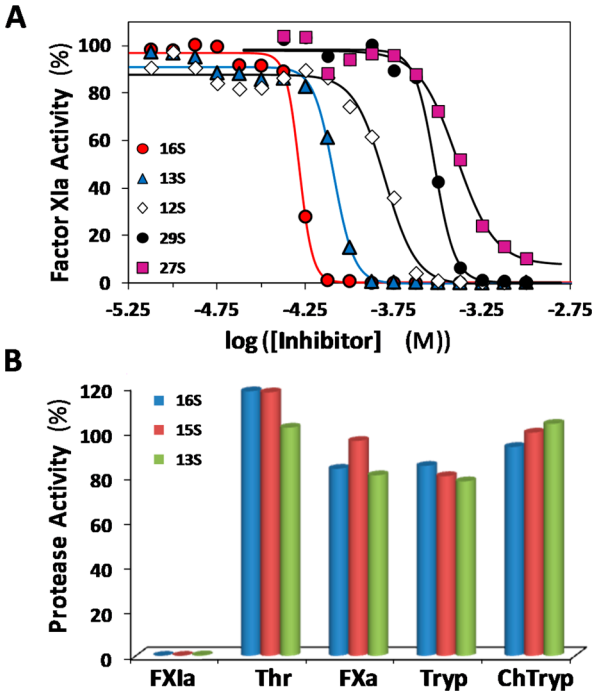

Figure 2. (A) Representative profiles of direct inhibition of human factor XIa (FXIa) by sulfated QAOs. The inhibition of FXIa was measured spectrophotometrically through a S2366 hydrolysis assay at pH 7.4 and 37 °C. Solid lines represent sigmoidal fits to the data to obtain IC_{50}, Y_M, and Y_0 using eq 1, as described in the Experimental Procedures. (B) Proteolytic activity of human thrombin (Thr), factor Xa (FXa), trypsin (Tryp), and chymotrypsin (ChTryp) by 500 μM sulfated QAO (**16S**, **15S**, and **13S**) using the chromogenic substrate assay. The assays were performed using substrates appropriate for the enzyme being studied under conditions closest to the physiological condition. The ratio of the proteolytic activity of an enzyme in the presence of the sulfated QAO to that in its absence was used to determine percent activity (%).

dependent "allosteric modulation". Molecules with only one sulfate group, that is, all monomeric sulfated QAOs and dimeric **7S**, were found to be inactive. Molecules containing two sulfate groups (**8S**−**17S**, **28S**, and **29S**) were most active (52−320 μM), while those with three or more sulfate groups (**18S**−**20S** and **25S**−**27S**) were progressively less potent (Tables 1 and 2). Among the inhibitors that contain two sulfate groups, those with $-OSO_3^-$ at the meta position on both rings are less potent than those with meta/para sulfate substitution, which in turn are less potent than para/para sulfate substitution. Comparative examples of the three categories include **9S**, **14S**, and **13S**, respectively, with affinities of 153, 91, and 82 μM (Table 1). That a sulfate group at the para position is favored is also borne out by comparison of **25S**, **26S**, and **27S** (Table 2). The observation that para substitution is more favored than either meta or ortho substitution is not unusual considering steric influence. Although the literature on sulfated, yet hydrophobic, small molecules is not extensive, our earlier work on sulfated benzofurans also suggests that the sterically most accessible 5-sulfate is the most preferred.[26,27]

Within the para/para disubstituted series, increasing the length of the linker from four (**13S**) to five (**15S**) to six methylenes (**16S**) increases the potency gradually (~80 → ~50 μM). The trend is also shown by the meta/meta disubstituted inhibitors **11S** (three atom linker) and **8S** (four atoms), which display IC_{50} values of 320 and 102 μM, respectively (Table 1). This is an unusual observation. Typically, conformational flexibility reduces the potency of inhibition. The result suggests that an extended linker probably serves to place the two QAO scaffolds better in two hydrophobic regions of FXIa. Comparison of **28S** and **16S** also supports this conclusion. Whereas **28S** contains two triazole rings, **15S** contains only one triazole moiety on an otherwise identical base scaffold. Both inhibitors contain a minimum of 10 linker atoms, yet the additional triazole of **28S** is likely to impart significant rigidity to the linker in comparison to that for **15S**. Inhibitor **28S** is approximately 6-fold less potent than **15S** (Tables 1 and 2).

Another factor that appears to play a role is the geometry of the triazole ring. Whereas 1,4-triazole containing **15S** displayed a potency of 59 μM, the potency dropped to 94 μM with **29S**, which contained a 1,5-triazole moiety. Likewise, nonsulfate substitutions, such as acetyl (e.g., **9S** and **19S**) or methoxy (e.g., **17S** and **26S**), also introduce variations in inhibitor potency suggesting a small but significant contribution of these positions in binding.

To assess whether the sulfated QAOs inhibited serine proteases related to human FXIa, we screened the inhibitors against thrombin, factor Xa, trypsin, and chymotrypsin. Screening was performed using appropriate chromogenic substrates, as described earlier.[28,31] Essentially, no inhibition was observed at concentrations as high as 500 μM (Figure 2B). This suggested high selectivity of sulfated QAOs for targeting human FXIa. This is not completely unexpected as the design strategy (Figure 1) should inherently engineer selectivity. Both the HBS and hP domain(s) are expected to be structurally different even on related enzymes; thus, engineering enhanced selectivity. In comparison, enzymes that possess only on one type of binding site (either HBS or hP) should not be targeted by sulfated QAOs.

Overall, the work led to identification of six inhibitors (**8S**, **13S**−**16S**, and **28S**) that displayed IC_{50} values less than 100 μM (Tables 1 and 2). All six molecules bear one sulfate group at either end of the molecule in a rather symmetric location. Molecules that are either more or less sulfated than these six are much less potent. The inhibition potency was significantly dependent on the substitution pattern of the sulfated QAO scaffold.

Comparison of Inhibition Potency of Sulfated QAOs With GAGs and GAG Mimetics. The best SAM discovered in this study, **16S**, displayed an IC_{50} of 52 μM (Table 1). This potency represents an excellent lead for the discovery of advanced molecules. Yet, this potency compares favorably to several sulfated molecules designed so far in the literature or available naturally. For example, rationally designed small mimetics of heparin pentasaccharide displayed antithrombin affinities in the range 10−1000 μM.[18,19,22,24,25] Similarly, a HS octasaccharide that recognizes herpes simplex virus glycoprotein D binds with an affinity of 19 μM.[37] Another GAG oligomer, that is, a dermatan sulfate (DS) hexasaccharide, binds to its target, heparin cofactor II, with an affinity of 20 μM.[38,39] Both these GAG oligomers, the HS octasaccharide and DS hexasaccharide, are thought to possess high selectivity for their targets and yet display relatively moderate affinities. We predict that rational optimization of **16S** through computational and/or structure-based approaches will yield significant increase in potency. Such approaches have in fact resulted in better GAG mimetics, as exemplified by the 1000-fold increase in potency shown by sulfated benzofurans dimers from their monomeric precursors.[26,40] Our recent report on sulfated pentagalloyl

dx.doi.org/10.1021/jm301757v | J. Med. Chem. XXXX, XXX, XXX−XXX

Table 1. Inhibition of Human Factor XIa by Sulfated QAOs 7S−20S[a]

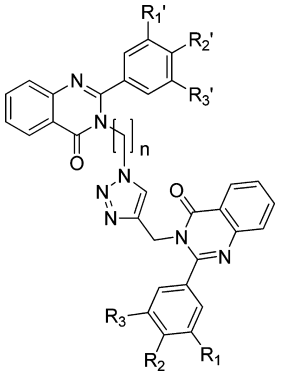

inhibitor	R_1	R_2	R_3	R_1'	R_2'	R_3'	n	IC_{50} (μM)	ΔY %
7S	−OAc	−H	−H	$-OSO_3^-$	−H	−H	4	>1000	NA[b]
8S	$-OSO_3^-$	−H	−H	$-OSO_3^-$	−H	−H	4	102 ± 2[c]	100 ± 6
9S	$-OSO_3^-$	−H	−OH	−OAc	−H	$-OSO_3^-$	4	153 ± 1	96 ± 1
10S	$-OCH_3$	$-OSO_3^-$	−H	$-OCH_3$	$-OSO_3^-$	−H	4	139 ± 1	95 ± 1
11S	$-OSO_3^-$	−H	−H	$-OSO_3^-$	−H	−H	3	320 ± 2	91 ± 4
12S	$-OSO_3^-$	−H	−H	−H	$-OSO_3^-$	−H	4	159 ± 2	88 ± 3
13S	−H	$-OSO_3^-$	−H	−H	$-OSO_3^-$	−H	4	82 ± 1	91 ± 2
14S	−H	$-OSO_3^-$	−H	$-OSO_3^-$	−H	−H	4	91 ± 2	103 ± 5
15S	−H	$-OSO_3^-$	−H	−H	$-OSO_3^-$	−H	5	59 ± 1	89 ± 2
16S	−H	$-OSO_3^-$	−H	−H	$-OSO_3^-$	−H	6	52 ± 1	97 ± 1
17S	$-OSO_3^-$	−H	−H	$-OCH_3$	$-OSO_3^-$	−H	4	182 ± 1	88 ± 5
18S	$-OSO_3^-$	−H	$-OSO_3^-$	$-OSO_3^-$	−H	−H	4	213 ± 2	93 ± 2
19S	$-OSO_3^-$	−H	$-OSO_3^-$	−OAc	−H	$-OSO_3^-$	4	273 ± 3	91 ± 2
20S	$-OSO_3^-$	−H	$-OSO_3^-$	$-OSO_3^-$	−H	$-OSO_3^-$	4	>1000	NA

[a]The IC_{50}, HS, and ΔY values were obtained following nonlinear regression analysis of direct inhibition of factor Xa. Inhibition was monitored by spectrophotometric measurement of residual proteases activity (see the Experimental Procedures). [b]Not applicable. [c]Errors represent ±1 SE.

Table 2. Inhibition of Human Factor XIa by Sulfated QAOs 25S−29S[a]

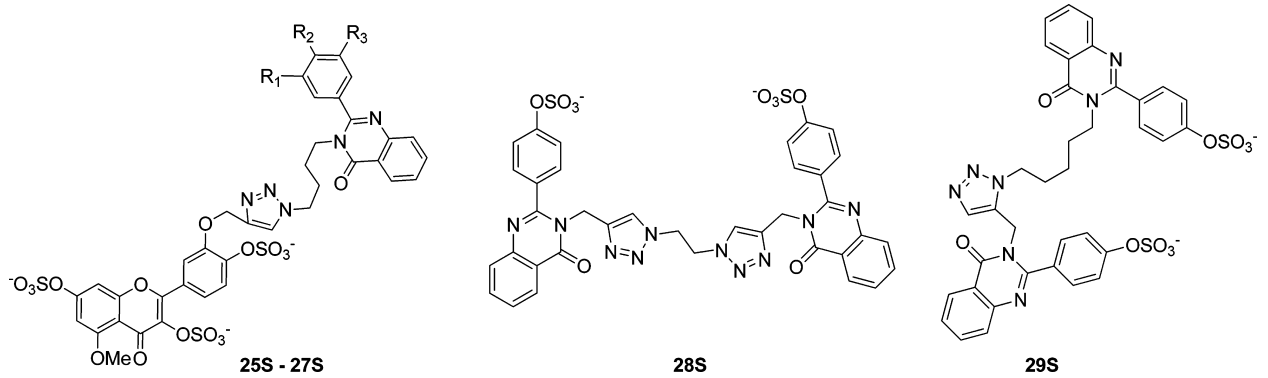

25S - 27S **28S** **29S**

inhibitor	R_1	R_2	R_3	IC_{50} (μM)	ΔY %
25S	$-OSO_3^-$	−H	−H	>1000	NA[b]
26S	$-OCH_3$	$-OSO_3^-$	−H	216 ± 27[c]	50 ± 13
27S	−OAc	−H	$-OSO_3^-$	407 ± 10	90 ± 6
28S	–	–	–	305 ± 3	98 ± 3
29S	–	–	–	90 ± 0.2	94 ± 1

[a]The IC_{50}, HS, and ΔY values were obtained following nonlinear regression analysis of direct inhibition of factor Xa. Inhibition was monitored by spectrophotometric measurement of residual proteases activity (see the Experimental Procedures). [b]Not applicable. [c]Errors represent ±1 SE.

glucoside inhibition of FXIa through its HBS also bodes well for design of second generation SAMs from the leads identified in this work.[41] A critical component to such an improvement would be the cocrystal structure of a SAM with human FXIa.[42]

Inhibition Potency of Sulfated QAOs in Human Plasma. To assess whether the chromogenic substrate-based inhibition of human factor XIa by sulfated QAOs translates into activity against macromolecular substrates, we studied anticoagulant activity in human plasma. Two assays, the prothrombin and activated partial thromboplastin time assays (PT and APTT, respectively), are typically utilized to identify an inhibitor's ability to retard the extrinsic and intrinsic

dx.doi.org/10.1021/jm301757v | J. Med. Chem. XXXX, XXX, XXX−XXX

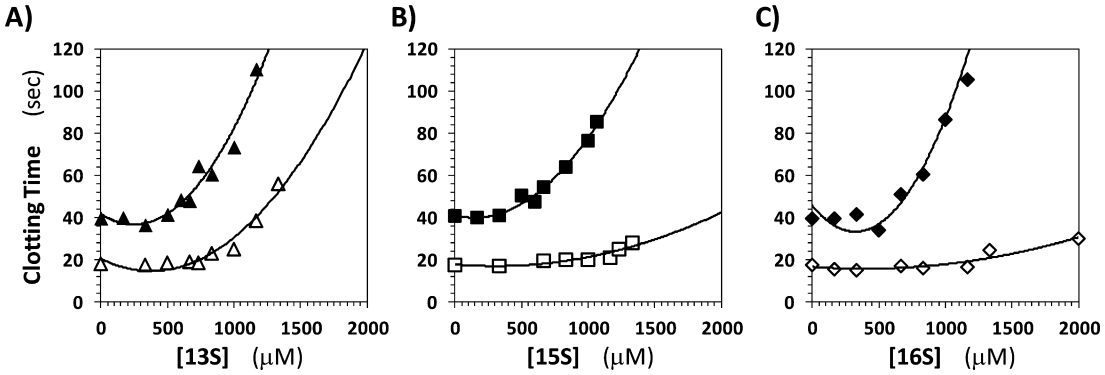

Figure 3. Human plasma anticoagulation by sulfated QAOs **13S** (A), **15S** (B), and **16S** (C). The time to clot was measured in either the APTT assay (solid symbols) or the PT assay (open symbols) in the presence of varying concentrations of the three sulfated QAOs. Solid lines are trend lines, which were used to calculate the concentration of the anticoagulant that is expected to double the clotting time. The mean of two experiments are reported.

coagulation signal. A dose-dependent prolongation of APTT is observed in the presence of sulfated QAOs **13S**, **15S**, and **16S** (Figure 3). A 2-fold increase in APTT was observed in the range 0.95−1.06 mM for the three molecules (Table 3), which

Table 3. Effect of Sulfated QAOs on Human Plasma Clotting Times[a]

inhibitor	2 × APTT (μM)	2 × PT (μM)
13S	979	1119
15S	1062	1684
16S	950	>2000

[a]Prolongation of clotting time as a function of concentration of sulfated quinazolinones in either the activated partial thromboplastin time assay (APTT) or the prothrombin time assay (PT). Clotting assays were performed in duplicate (SE ≤ 10%) as described in the Experimental Procedures.

is about 12−18-fold less active in comparison to the potency in buffer. This is typical of many anticoagulants and arises primarily from binding to human serum albumin.[43,44] In the PT assay, only **13S** appears to exhibit reasonable dose-dependent prolongation of clotting time with a 2-fold increase calculated to occur at about 1.12 mM. Inhibitors **15S** and **16S** are much less active in the PT assay. Although the coagulation cascade is a highly intertwined network of proteolytic reactions, it is generally accepted that the primary effect of FXIa is in the intrinsic pathway. This implies that inhibition of FXIa is likely to more dramatically affect the APTT in comparison to the PT. Thus, the results observed for **15S** and **16S** further support the selective inhibition of FXIa. The effect of **13S** on both the APTT and PT is interesting and intriguing and requires further experimental study.

Mechanism of Inhibition of Sulfated QAOs. Inherent in the design strategy is the expectation that SAMs should function as allosteric modifiers of proteolytic activity. To assess this, the kinetics of chromogenic substrate S2366 hydrolysis by factor XIa in the presence of **14S** was studied. The plot of initial rate as a function of Spectrozyme FXIa concentration displayed a characteristic hyperbolic profile (Figure 4), which was fitted using the standard Michaelis−Menten equation to derive the K_M and V_{max} of factor XIa activity. The K_M for Spectrozyme FXIa was found to be 0.31 ± 0.03 mM, which did not change much as the concentration of **14S** increased to 135 μM (0.30 ± 0.07 mM). In constrast, the V_{max} decreased from 43.3 ± 1.5 to

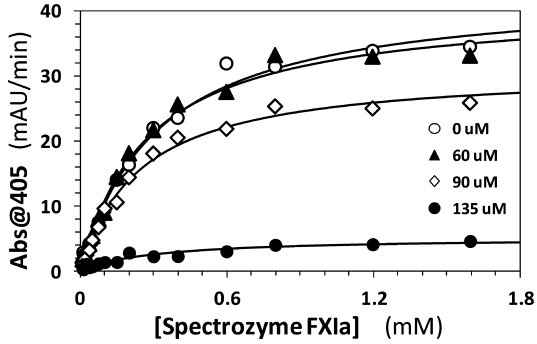

Figure 4. Michaelis−Menten kinetics of S2366 hydrolysis by human factor XIa in the presence of sulfated QAO **14S**. The initial rate of hydrolysis at various substrate concentrations was measured spectrophotometrically in pH 7.4 buffer at 37 °C. Solid lines represent nonlinear regressional fits to the data by the standard Michaelis−Menten equation to yield K_M and V_{max}.

5.1 ± 0.5 mAU/min as the concentration of **14S** increased from 0 to 135 μM. Thus, while the affinity of small chromogenic substrate remains unaffected by **14S** binding, the proteolytic activity decreases. This is characteristic of a noncompetitive mechanism of factor XIa inhibition, and most H/HS mimetics reported in the literature to date, such as sulfated low molecular weight lignins[45] and sulfated benzofurans,[26,40] have exhibited such a mechanism.

Sulfated QAOs Engage Residues of the HBS Present on the Catalytic Domain of Factor XIa. Heparin binds to FXIa in two sites, in the A3 domain (Lys252, Lys253, and Lys255) and in the catalytic domain (Lys529, Arg530, Arg532, Lys535, and Lys539). To identify whether sulfated QAOs engage the A3 domain or the catalytic domain, we studied inhibition of human FXIa containing only the catalytic domain. This domain and all site-directed mutants were expressed and purified, as described earlier.[32,33] The catalytic domain alone (FXIa-CD) was inhibited by a sulfated QAO, **16S**, as potently as the wild-type enzyme indicating that the A3 domain is not necessary for activity (not shown). Replacement of Arg530 alone by Ala in FXIa-CD resulted in an increase of 2-fold in the IC_{50} (Figure 5). Further replacement of Lys529, Arg530, and Arg532 to Ala each reduced the potency by approximately 5-fold (Figure 5). At the same time, Lys535Ala and Lys539Ala exhibited no change in the IC_{50} of **16S** from that of the wild-type FXIa-CD (not shown). This implies that one or more

dx.doi.org/10.1021/jm301757v | J. Med. Chem. XXXX, XXX, XXX−XXX

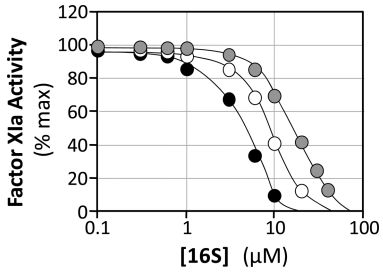

Figure 5. Dose–response profiles for **16S** inhibition of recombinant wild-type FXIa catalytic domain (FXIa-CD, solid circles), Arg530Ala FXIa-CD single mutant (open circles), and Lys529Ala/Arg530Ala/Arg532Ala FXIa-CD triple mutant (shaded circles) in 50 mM Tris–HCl buffer pH 7.4 containing 150 mM NaCl, 0.1% PEG8000, and 0.02% Tween80 at 37 °C. Solid lines represent sigmoidal dose–response fits of eq 1.

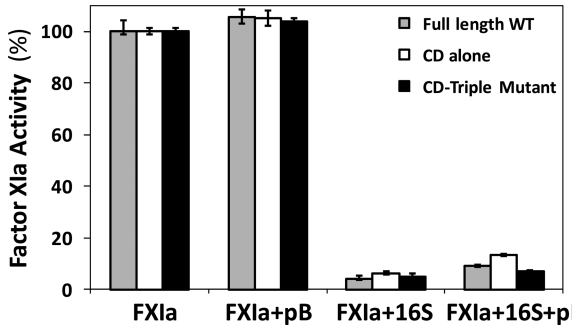

Figure 6. Effect of Polybrene on the proteolytic activity of full-length wild-type factor XIa (shaded bars), FXIa-CD (open bars), and FXIa-CD containing Lys529Ala/Arg530Ala/Arg532Ala triple mutations (solid bars). The proteolytic activities of each enzyme in the presence of 30 μM Polybrene and 3 μM **16S** were measured using S2366 hydrolysis. See the text for details.

residues of the HBS present on the catalytic domain of FXIa is(are) involved in binding to **16S**. The loss of affinity for **16S** with the triple mutation is moderate. In comparison, replacement of a single arginine on thrombin (Arg173) introduced a defect of approximately 22-fold for a sulfated benzofuran,[27] while for sulfated low molecular weight lignins, the loss in potency was in the range 2–8-fold.[28] This implies that the loss in potency for sulfated QAOs is more similar to that of sulfated low molecular weight lignins than that for sulfated benzofurans. Sulfated lignins contain several sulfate groups, which bind to more than one arginine/lysine residues on thrombin.[28] In a similar manner, the two sulfate groups of QAOs likely bind to two arginine/lysine loci on factor XIa. The site-directed mutagenesis data shows that one of these electropositive loci is the HBS. The other locus remains to be identified. In combination with the noncompetitive mechanism of inhibition, the results suggest that sulfated QAOs recognize an exosite on FXIa away from the active site or allosterically inhibit the enzyme.

Factor XIa Inhibition by Sulfated QAOs Is Not Neutralized by a Competing Electropositive Polymer. A critical element of the proposed design principle is that hP domain(s) on the target enzyme are involved in selective inhibition. To assess this aspect, we studied the effect of Polybrene on the proteolytic activity of factor XIa. Polybrene has been regularly used to neutralize heparin since the early 1990s.[46,47] Basically, the multiple positive charges of Polybrene neutralize the numerous sulfate and carboxylate groups of heparin resulting in an antidote effect. If sulfated QAOs bind to factor XIa only through electrostatic sulfate–arginine/lysine forces and not through significant hydrophobic forces, then Polybrene should neutralize their inhibitory effects. Figure 6 shows the **16S** inhibition of the catalytic activity of wild-type FXIa, FXIa-CD, and FXIa-CD containing triple mutation (Lys529Ala/Arg530Ala/Arg532Ala) in the presence of Polybrene. The proteolytic activity of both the full length, wild-type FXIa, FXIa-CD, and FXIa-CD containing triple mutations is reduced to 4.2 ± 1.0, 6.3 ± 0.7, and 4.9 ± 1.2%, respectively, in the presence of **16S**. This is as expected due to saturation of FXIa by **16S**. Addition of 30 μM Polybrene, which rapidly neutralizes heparin's anticoagulant effect, changes the inhibition level to 9.2 ± 0.2% (wild-type FXIa), 13.1 ± 0.4% (FXIa-CD), and 7.1 ± 0.1% (FXIa-CD with triple mutations). The reduction in inhibition shows that the antidote does affect FXIa–**16S** interaction, but the influence is mostly marginal. A primarily electrostatic interaction between FXIa and **16S** should have been nearly fully reversed by the high concentration of Polybrene. Thus, **16S** appears to utilize primarily hydrophobic forces in binding to FXIa. Also evident from these results is the role of the HBS residues. The loss in inhibition by the addition of Polybrene is nearly 2-fold for full length, wild-type FXIa and FXIa-CD but is 1.45-fold for the FXIa-CD with triple mutations. This implies that, when a small group of positively charged residues are eliminated, the contribution of electrostatic forces decreases, as expected. Both of these aspects are key elements of the proposed design principle and are expected to contribute to the selectivity observed in targeting FXIa (above). Yet, these results should be tempered with the recognition that Polybrene is not selective for sulfated QAO. Unfortunately, no agent is currently available that can selectively compete with such sulfated and yet hydrophobic molecules. The best avenue for establishing the proposed dual-element design strategy is likely to be X-ray structure determination of a FXIa–SAM cocomplex.

Sulfated QAOs Bind to Factor XIa in a Classic, Direct Allosteric Manner. The studies performed so far indicate that sulfated QAO inhibit human FXIa by utilizing an allosteric site. However, the HBS on the catalytic domain of FXIa, although allosteric, is within 22 Å of the active site. The molecular size of sulfated QAOs is also fairly large raising a minor concern whether the inhibition is truly through an allosteric, cooperative process. To test this possibility, we studied the interaction of sulfated QAOs with FXIa irreversibly blocked at the active site using a dansylated EGR peptide, that is, FXIa-DEGR. Figure 7A shows the fluorescence emission spectra of FXIa alone and in complex with a SAM (**13S–16S**). The fluorescence of the active site dansyl group increases in the presence of each sulfated QAO. The maximal increase in fluorescence is dependent on the type of sulfated QAO. In addition, the emission maximum of FXIa-DEGR shifts from approximately 550 nm in the absence of sulfated QAOs to ~505 nm in their presence suggesting a major blueshift. Both the increase in fluorescence intensity and the blueshift in λ_{em} suggest strong perturbation of the electrostatic environment around the active site of FXIa following interaction with sulfated QAOs.

To further investigate the interaction, the fluorescence of FXIa-DEGR was monitored as a function of sulfated QAO concentration. Figure 7B shows the profiles of the titrations for the most potent sulated QAOs **13S–16S**. The profiles reveal a characteristic sigmoidal dependence on the concentration of sulfated QAO. This is a striking observation and strongly

dx.doi.org/10.1021/jm301757v | J. Med. Chem. XXXX, XXX, XXX–XXX

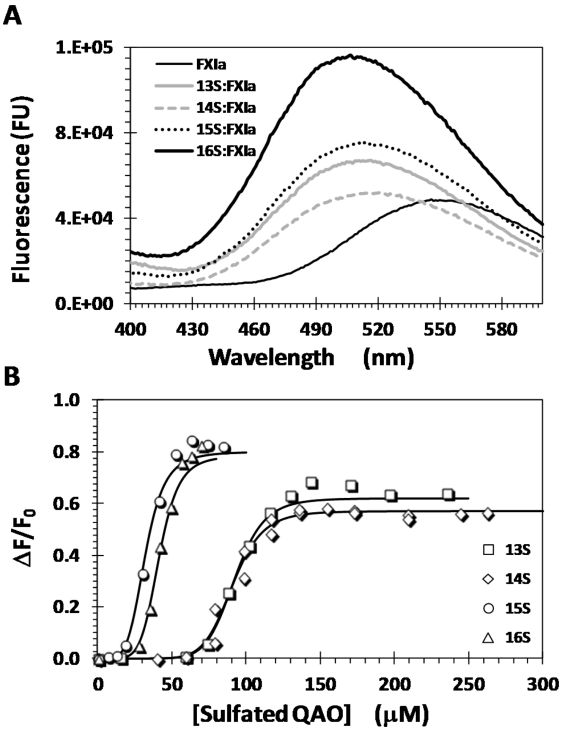

Figure 7. (A) Changes in the fluorescence emission spectrum of dansylated factor XIa (FXIa-DEGR) induced by the binding of sulfated QAOs. Spectra were recorded in 50 mM Tris−HCl buffer of pH 7.4 containing 150 mM NaCl and 0.1% PEG8000 at 37 °C. (B) Fractional change in fluorescence of FXIa-DEGR at 547 nm (λ_{ex} = 345 nm) as a function of the concentration of sulfated QAOs (**13S−16S**). Solid line represents nonlinear regressional fit to the data using the standard Hill eq 3 to obtain the ΔF_{max}, Hill coefficient "*n*", and K_D of binding.

suggestive of a cooperative binding process. The profile can be fitted well by the standard, three-parameter Hill equation, which gives the maximal fluorescence change (ΔF_{max}), the Hill coefficient (n), and the apparent dissociation constant (K_D) of binding (Table 4). By using this equation, the four sulfated QAOs were found to bind with an affinity of 37−91 μM, which compare favorably with the IC_{50} measured above. The Hill coefficients were calculated to be in the range 6.4−9.0, which support a strongly cooperative, allosteric interaction. Overall, the thermodynamic fluorescence study demonstrates that sulfated QAOs bind to FXIa through a classic, allosteric interaction process.

Table 4. Thermodynamics of Sulfated QAOs Binding to Human FXIa[a]

inhibitor	ΔF_{max} (%)	n	K_D (μM)
13S	66 ± 2[b]	7.9 ± 1.9	84 ± 12
14S	57 ± 2	9.0 ± 1.1	91 ± 2
15S	72 ± 2	6.8 ± 2.7	37 ± 8
16S	90 ± 3	6.4 ± 2.0	38 ± 5

[a]Titrations were performed by adding aliquots of a solution of sulfated QAOs (**13S−16S**) to 250 nM FXIa−DEGR in 50 mM Tris−HCl buffer of pH 7.4 containing 150 mM NaCl and 0.1% PEG8000 at 37 °C and monitoring the change in the fluorescence of FXIa−DEGR at 547 nm (λ_{EX} = 345 nm). The ΔF_{max}, the Hill coefficient "*n*", and K_D were obtained by nonlinear regressional fit of the data by eq 3. [b]Error = ± 1 SE.

SIGNIFICANCE

Human FXIa is a key coagulation protease and is being increasingly regarded as the most optimal enzyme to target for developing new antithrombotics that are devoid of bleeding consequences.[32,33,48,49] Studies show that reducing the levels of active FXI significantly reduces clotting tendency. Most importantly, this reduction in activity leaves the normal hemostasis unaffected. Additionally, ischemic stroke, a deleterious effect, is significantly reduced in FXI-deficient patients. In contrast, venous thrombosis arises from higher natural levels of FXI. Thus, the sulfated QAOs discovered in this work will be key leads in designing more potent inhibitors of an enzyme thought to be safer to target.

To date, only a handful of small molecule inhibitors of FXIa have been reported. These molecules are orthosteric, active site directed inhibitors.[50−56] Among these, the reversible inhibitors contain a strongly basic group that recognizes the active site Asp189 of FXIa. In contrast, the irreversible inhibitors covalently target the active site Ser195 through the use of boronic acid or ketothiazole groups. Sulfated QAOs are significant because these function through an allosteric site. Recently, we reported the first allosteric inhibitor of human FXIa, sulfated pentagalloyl glucoside, that directly binds to one of the enzyme's HBSs.[41] The two allosteric inhibitors, sulfated QAO and sulfated pentagalloyl glucoside, are structurally completely different and appear to utilize different allosteric sites. This implies that multiple opportunities are available for exploiting allosteric inhibition of FXIa. In comparison to orthosteric inhibition, allosteric modulation of an enzyme's activity offers the promise of controlling the efficacy of inhibition (ΔY). For example, inhibitor **26S** displays only 50% efficacy, while **13S−16S** display efficacy greater than 85% (Tables 1 and 2). This implies that it may be possible to design new sulfated QAOs with variable levels of efficacies that likely offer a finer control over the anticoagulation state of plasma.

The discovery of sulfated QAOs, in combination with work on sulfated benzofurans,[26,27] supports the dual-element design concept present in Figure 1. This is a simple approach, amenable to computational modeling, and likely to be very useful. A major promise of this approach is high target selectivity. Because GAGs primarily function through exosites, the proposed SAM design strategy is expected to be applicable to many GBPs such as serpins, growth factors, chemokines, and viral envelope glycoproteins.

ASSOCIATED CONTENT

Supporting Information

General procedures for the synthesis of polyphenolic quinazolin-4(3H)-ones **3a−3g**, **7−20**, and **25−29** and other intermediate compounds. ^{1}H and ^{13}C NMR spectra and HRMS spectra for select compounds. This material is available free of charge via the Internet at http://pubs.acs.org.

AUTHOR INFORMATION

Corresponding Author

*Phone: (804) 828-7328; fax: (804) 827-3664; e-mail: urdesai@vcu.edu.

Notes

The authors declare no competing financial interest.

dx.doi.org/10.1021/jm301757v | J. Med. Chem. XXXX, XXX, XXX−XXX

■ ACKNOWLEDGMENTS

This work was supported by grants HL090586 and HL107152 from the National Institutes of Health to U.R.D.

■ ABBREVIATIONS USED

APTT, activated partial thromboplastin time; CuAAC, copper-catalyzed azide−alkyne cycloaddition reaction; DS, dermatan sulfate; FXI, factor XI; FXIa, factor XIa; FXIa−CD, catalytic domain of FXIa; FXIIIa, factor XIIIa; GAG, glycosaminoglycan; GBP, GAG-binding protein; HBS, heparin-binding site; hP, hydrophobic; HS, heparan sulfate; QAO, quinazolin-4(3H)-ones; PEG, polyethylene glycol; PT, prothrombin time; SAM, sulfated allosteric modulator

■ REFERENCES

(1) Sarrazin, S.; Lamanna, W. C.; Esko, J. D. Heparan sulfate proteoglycans. *Cold Spring Harbor Perspect. Biol.* **2011**, *3*, a004952.
(2) Maeda, N.; Ishii, M.; Nishimura, K.; Kamimura, K. Functions of chondroitin sulfate and heparan sulfate in the developing brain. *Neurochem. Res.* **2011**, *36*, 1228−1240.
(3) Olson, S. T.; Richard, B.; Izaguirre, G.; Schedin-Weiss, S.; Gettins, P. G. Molecular mechanisms of antithrombin-heparin regulation of blood clotting proteinases. A paradigm for understanding proteinase regulation by serpin family protein proteinase inhibitors. *Biochimie* **2010**, *92*, 1587−1596.
(4) Gandhi, N. S.; Mancera, R. L. The structure of glycosaminoglycans and their interactions with proteins. *Chem. Biol. Drug Des.* **2008**, *72*, 455−482.
(5) Desai, U. R. New antithrombin-based anticoagulants. *Med. Res. Rev.* **2004**, *24*, 151−181.
(6) Kreuger, J.; Spillmann, D.; Lindahl, U. Interactions between heparan sulfate and proteins: the concept of specificity. *J. Cell Biol.* **2006**, *174*, 323−327.
(7) Lindahl, U. Heparan sulfate-protein interactions − A concept for drug design. *Thromb. Haemostasis* **2007**, *98*, 109−115.
(8) Mosier, P. D.; Krishnasamy, C.; Kellogg, G. E.; Desai, U. R. On the specificity of heparin/heparan sulfate binding to proteins. Anion-binding sites on antithrombin and thrombin are fundamentally different. *PLoS One* **2012**, *7*, e48632.
(9) Coulomb forces have a r^{-1} (r = distance between two ions) relationship, whereas van der Waals forces have a r^{-3} to r^{-6} dependence.
(10) Petitou, M.; Nancy-Portebois, V.; Dubreucq, G.; Motte, V.; Meuleman, D.; de Kort, M.; van Boeckel, C. A.; Vogel, G. M.; Wisse, J. A. From heparin to EP217609: The long way to a new pentasaccharide-based neutralisable anticoagulant with an unprecedented pharmacological profile. *Thromb. Haemostasis* **2009**, *102*, 804−810.
(11) Saxena, K.; Schieborr, U.; Anderka, O.; Duchardt-Ferner, E.; Elshorst, B.; Gande, S. L.; Janzon, J.; Kudlinzki, D.; Sreeramulu, S.; Dreyer, M. K.; Wendt, K. U.; Herbert, C.; Duchaussoy, P.; Bianciotto, M.; Driguez, P. A.; Lassalle, G.; Savi, P.; Mohammadi, M.; Bono, F.; Schwalbe, H. Influence of heparin mimetics on assembly of the FGF·FGFR4 signaling complex. *J. Biol. Chem.* **2010**, *285*, 26628−26640.
(12) Sarrazin, S.; Bonnaffé, D.; Lubineau, A.; Lortat-Jacob, H. Heparan sulfate mimicry: A synthetic glycoconjugate that recognizes the heparin binding domain of interferon-gamma inhibits the cytokine activity. *J. Biol. Chem.* **2005**, *280*, 37558−37564.
(13) Lubineau, A.; Lortat-Jacob, H.; Gavard, O.; Sarrazin, S.; Bonnaffé, D. Synthesis of tailor-made glycoconjugate mimetics of heparan sulfate that bind IFN-γ in the nanomolar range. *Chem.—Eur. J.* **2004**, *10*, 4265−4282.
(14) Ferro, V.; Dredge, K.; Liu, L.; Hammond, E.; Bytheway, I.; Li, C.; Johnstone, K.; Karoli, T.; Davis, K.; Copeman, E.; Gautam, A. PI-88 and novel heparan sulfate mimetics inhibit angiogenesis. *Semin. Thromb. Hemostasis* **2007**, *33*, 557−568.
(15) Nimjee, S. M.; Oney, S.; Volovyk, Z.; Bompiani, K. M.; Long, S. B.; Hoffman, M.; Sullenger, B. A. Synergistic effect of aptamers that inhibit exosites 1 and 2 on thrombin. *RNA* **2009**, *15*, 2105−2111.
(16) Freeman, C.; Liu, L.; Banwell, M. G.; Brown, K. J.; Bezos, A.; Ferro, V.; Parish, C. R. Use of sulfated linked cyclitols as heparan sulfate mimetics to probe the heparin/heparan sulfate binding specificity of proteins. *J. Biol. Chem.* **2005**, *280*, 8842−8849.
(17) Türk, H.; Haag, R.; Alban, S. Dendritic polyglycerol sulfates as new heparin analogues and potent inhibitors of the complement system. *Bioconjugate Chem.* **2004**, *15*, 162−167.
(18) Gunnarsson, G. T.; Desai, U. R. Interaction of designed sulfated flavanoids with antithrombin: Lessons on the design of organic activators. *J. Med. Chem.* **2002**, *45*, 4460−4470.
(19) Gunnarsson, G. T.; Desai, U. R. Designing small, nonsugar activators of antithrombin using hydropathic interaction analyses. *J. Med. Chem.* **2002**, *45*, 1233−1243.
(20) Correia-da-Silva, M.; Sousa, E.; Duarte, B.; Marques, F.; Cunha-Ribeiro, L. M.; Pinto, M. M. Dual anticoagulant/antiplatelet persulfated small molecules. *Eur. J. Med. Chem.* **2011**, *46*, 2347−2358.
(21) Correia-da-Silva, M.; Sousa, E.; Duarte, B.; Marques, F.; Carvalho, F.; Cunha-Ribeiro, L. M.; Pinto, M. M. Flavonoids with an oligopolysulfated moiety: A new class of anticoagulant agents. *J. Med. Chem.* **2011**, *54*, 95−106.
(22) Gunnarsson, G. T.; Riaz, M.; Adams, J.; Desai, U. R. Synthesis of per-sulfated flavonoids using 2,2,2-trichloro ethyl protecting group and their factor Xa inhibition potential. *Bioorg. Med. Chem.* **2005**, *13*, 1783−1789.
(23) Correia-da-Silva, M.; Sousa, E.; Duarte, B.; Marques, F.; Carvalho, F.; Cunha-Ribeiro, L. M.; Pinto, M. M. Polysulfated xanthones: Multipathway development of a new generation of dual anticoagulant/antiplatelet agents. *J. Med. Chem.* **2011**, *54*, 5373−5384.
(24) Al-Horani, R. A.; Liang, A.; Desai, U. R. Designing nonsaccharide, allosteric activators of antithrombin for accelerated inhibition of factor Xa. *J. Med. Chem.* **2011**, *54*, 6125−6138.
(25) Raghuraman, A.; Liang, A.; Krishnasamy, C.; Lauck, T.; Gunnarsson, G. T.; Desai, U. R. On designing non-saccharide, allosteric activators of antithrombin. *Eur. J. Med. Chem.* **2009**, *44*, 2626−2631.
(26) Sidhu, P. S.; Liang, A.; Mehta, A. Y.; Abdel Aziz, M. H.; Zhou, Q.; Desai, U. R. Rational design of potent, small, synthetic allosteric inhibitors of thrombin. *J. Med. Chem.* **2011**, *54*, 5522−5531.
(27) Abdel Aziz, M. H.; Sidhu, P. S.; Liang, A.; Kim, J. Y.; Mosier, P. D.; Zhou, Q.; Farrell, D. H.; Desai, U. R. Designing allosteric regulators of thrombin. Monosulfated benzofuran dimers selectively interact with arg173 of exosite II to induce inhibition. *J. Med. Chem.* **2012**, *55*, 6888−6897.
(28) Abdel Aziz, M. H.; Mosier, P. D.; Desai, U. R. Identification of the site of binding of sulfated, low molecular weight lignins on thrombin. *Biochem. Biophys. Res. Commun.* **2011**, *413*, 348−352.
(29) Al-Horani, R. A.; Desai, U. R. Chemical sulfation of small molecules-advances and challenges. *Tetrahedron* **2010**, *66*, 2907−2918.
(30) Raghuraman, A.; Riaz, M.; Hindle, M.; Desai, U. R. Rapid and efficient microwave-assisted synthesis of highly sulfated organic scaffolds. *Tetrahedron Lett.* **2007**, *48*, 6754−6758.
(31) Henry, B. L.; Thakkar, J. N.; Liang, A.; Desai, U. R. Sulfated, low molecular weight lignins inhibit a select group of heparin-binding serine proteases. *Biochem. Biophys. Res. Commun.* **2012**, *417*, 382−386.
(32) Smith, S. B.; Gailani, D. Update on the physiology and pathology of factor IX activation by factor XIa. *Expert Rev. Hematol.* **2008**, *1*, 87−98.
(33) Emsley, J.; McEwan, P. A.; Gailani, D. Structure and function of factor XI. *Blood* **2010**, *115*, 2569−2577.
(34) Xia, Y.; Yang, Z. Y.; Hour, M. J.; Kuo, S. C.; Xia, P.; Bastow, K. F.; Nakanishi, Y.; Nampoothiri, P.; Hackl, T.; Hamel, E.; Lee, K. H. Antitumor agents. Part 204: Synthesis and biological evaluation of 2-aryl quinazolinones. *Bioorg. Med. Chem. Lett.* **2001**, *11*, 1193−1196.
(35) Rostovtsev, V. V.; Green, L. G.; Fokin, V. V.; Sharpless, K. B. A stepwise Huisgen cycloaddition process: Copper(I)-catalyzed regiose-

lective "ligation" of azides and terminal alkynes. *Angew. Chem., Int. Ed.* **2002**, *41*, 2596−2599.
(36) Zhang, Li.; Chen, X.; Xue, P.; Sun, H. H. Y.; Williams, I. D.; Sharpless, K. B.; Fokin, V. V.; Jia, G. Ruthenium-catalyzed cycloaddition of alkynes and organic azides. *J. Am. Chem. Soc.* **2005**, *127*, 15998−15999.
(37) Copeland, R.; Balasubramaniam, A.; Tiwari, V.; Zhang, F.; Bridges, A.; Linhardt, R. J.; Shukla, D.; Liu, J. Using a 3-*O*-sulfated heparin octasaccharide to inhibit the entry of herpes simplex virus type 1. *Biochemistry* **2008**, *47*, 5774−5783.
(38) Tollefsen, D. M. The interaction of glycosaminoglycans with heparin cofactor II: Structure and activity of a high-affinity dermatan sulfate hexasaccharide. *Adv. Exp. Med. Biol.* **1992**, *313*, 167−176.
(39) Raghuraman, A.; Mosier, P. D.; Desai, U. R. Understanding dermatan sulfate-heparin cofactor II interaction through virtual library screening. *ACS Med. Chem. Lett.* **2010**, *1*, 281−285.
(40) Verghese, J.; Liang, A.; Sidhu, P. S.; Hindle, M.; Zhou, Q.; Desai, U. R. First steps in the direction of synthetic, allosteric, direct inhibitors of thrombin and factor Xa. *Bioorg. Med. Chem. Lett.* **2009**, *19*, 4126−4129.
(41) Al-Horani, R. A.; Ponnusamy, P.; Mehta, A. Y.; Gailani, D.; Desai, U. R. Sulfated pentagalloylglucoside is a potent, allosteric, and selective inhibitor of factor XIa. *J. Med. Chem.* **2013**, *56*, 867−878.
(42) Jin, L.; Pandey, P.; Babine, R. E.; Gorga, J. C.; Seidl, K. J.; Gelfand, E.; Weaver, D. T.; Abdel-Meguid, S. S.; Strickler, J. E. Crystal structures of the FXIa catalytic domain in complex with ecotin mutants reveal substrate-like interactions. *J. Biol. Chem.* **2005**, *280*, 4704−4712.
(43) Yacobi, A.; Udall, J. A.; Levy, G. Serum-protein binding as a determinant of warfarin body clearance and anticoagulant effect. *Clin. Pharmacol. Ther.* **1976**, *19*, 552−558.
(44) Kragh-Hansen, U. Structure and ligand binding properties of human serum albumin. *Dan. Med. Bull.* **1990**, *37*, 57−84.
(45) Henry, B. L.; Monien, B. H.; Bock, P. E.; Desai, U. R. A novel allosteric pathway of thrombin inhibition. Exosite II mediated potent inhibition of thrombin by chemo-enzymatic, sulfated dehydropolymers of 4-hydroxycinnamic acids. *J. Biol. Chem.* **2007**, *282*, 31891−31899.
(46) Rotteveel, R. C.; Roozendaal, K. J.; Weijers, R. N.; Eijsman, L. Influence of heparin, protamine and Polybrene on the time integral of thrombin generation (endogenous thrombin potential). *Haemostasis* **1996**, *26*, 1−10.
(47) Harsfalvi, J.; Pfliegler, G.; Udvardy, M.; Boda, Z.; Tornai, I.; Rak, K. The use of Polybrene for heparin neutralization in protein C activity assay. *Blood Coagulation Fibrinolysis* **1990**, *1*, 357−361.
(48) Goto, S. Factor XIa as a possible new target of antithrombotic therapy. *J. Thromb. Haemostasis* **2006**, *4*, 1494−1495.
(49) Schumacher, W. A.; Luettgen, J. M.; Quan, M. L.; Seiffert, D. A. Inhibition of Factor Xia as a new approach to anticoagulation. *Arterioscler., Thromb., Vasc. Biol.* **2010**, *30*, 388−392.
(50) Wong, P. C.; Crain, E. J.; Watson, C. A.; Schumacher, W. A. A small-molecule factor XIa inhibitor produces antithrombotic efficacy with minimal bleeding time prolongation in rabbits. *J. Thromb. Thrombolysis* **2011**, *32*, 129−137.
(51) Lin, J.; Deng, H.; Jin, L.; Pandey, P.; Quinn, J.; Cantin, S.; Rynkiewicz, M. J.; Gorga, J. C.; Bibbins, F.; Celatka, C. A.; Nagafuji, P.; Bannister, T. D.; Meyers, H. V.; Babine, R. E.; Hayward, N. J.; Weaver, D.; Benjamin, H.; Stassen, F.; Abdel-Meguid, S. S.; Strickler, J. E. Design, synthesis, and biological evaluation of peptidomimetic inhibitors of factor XIa as novel anticoagulants. *J. Med. Chem.* **2006**, *49*, 7781−7791.
(52) Deng, H.; Bannister, T. D.; Jin, L.; Babine, R. E.; Quinn, J.; Nagafuji, P.; Celatka, C. A.; Lin, J.; Lazarova, T. I.; Rynkiewicz, M. J.; Bibbins, F.; Pandey, P.; Gorga, J. C.; Meyers, H. V.; Abdel-Meguid, S. S.; Strickler, J. E. Synthesis, SAR exploration, and X-ray crystal structures of factor XIa inhibitors containing an α-ketothiazole arginine. *Bioorg. Med. Chem. Lett.* **2006**, *16*, 3049−3054.
(53) Lazarova, T. I.; Jin, L.; Rynkiewicz, M.; Gorga, J. C.; Bibbins, F.; Meyers, H. V.; Babine, R.; Strickler, J. Synthesis and in vitro biological evaluation of aryl boronic acids as potential inhibitors of factor XIa. *Bioorg. Med. Chem. Lett.* **2006**, *16*, 5022−5027.
(54) Schumacher, W. A.; Seiler, S. E.; Steinbacher, T. E.; Stewart, A. B.; Bostwick, J. S.; Hartl, K. S.; Liu, E. C.; Ogletree, M. L. Antithrombotic and hemostatic effects of a small molecule factor Xia inhibitor in rats. *Eur. J. Pharmacol.* **2007**, *570*, 167−174.
(55) Buchanan, M. S.; Carroll, A. R.; Wessling, D.; Jobling, M.; Avery, V. M.; Davis, R. A.; Feng, Y.; Xue, Y.; Oster, L.; Fex, T.; Deinum, J.; Hooper, J. N.; Quinn, R. J.; Clavatadine, A. A natural product with selective recognition and irreversible inhibition of factor XIa. *J. Med. Chem.* **2008**, *51*, 3583−3587.
(56) Hanessian, S.; Larsson, A.; Fex, T.; Knecht, W.; Blomberg, N. Design and synthesis of macrocyclic indoles targeting blood coagulation cascade Factor XIa. *Bioorg. Med. Chem. Lett.* **2010**, *20*, 6925−6928.